의학석사 학위논문

NSDHL 유전자가 유방암 증식과 전이에 미치는 영향 및 그 기전 연구

NAD(P)−dependent steroid dehydrogenase−like, involved in cholesterol biosynthesis, regulates proliferation and metastasis in breast cancer

2019년 2월

서울대학교 대학원

협동과정 종양생물학 전공

윤 소 현

NSDHL 유전자가 유방암 증식과 전이에 미치는 영향 및 그 기전 연구

NAD(P)-dependent steroid dehydrogenase-like, involved in cholesterol biosynthesis, regulates proliferation and metastasis in breast cancer

February 2019

Seoul National University

Cancer Biology

So-Hyun Yoon

NSDHL 유전자가 유방암 증식과 전이에 미치는 영향 및 그 기전 연구

지도교수 한 원 식

이 논문을 의학석사 학위논문으로 제출함

2018년 10월

서울대학교 대학원

협동과정 종양생물학 전공

윤 소 현

윤소현의 의학석사 학위논문을 인준함

2018년 12월

위 원 장 임 석 아 (인)

부 위 원 장 한 원 식 (인)

위 원 석 승 혁 (인)

NAD(P)−dependent steroid dehydrogenase−like, involved in cholesterol biosynthesis, regulates proliferation and metastasis in breast cancer

by

So−Hyun Yoon

A Thesis Submitted to the Interdisciplinary Graduate Program

in Partial Fulfillment of the Requirements

for the Degree of Master of Science in Medicine

in Cancer Biology at Seoul National University

Seoul, Korea

December 2018

Approved by Thesis Committee

Professor _____ , Chair

Professor _____ , Vice Chairman

Professor _____

Abstract

NAD(P)-dependent steroid dehydrogenase-like, involved in cholesterol biosynthesis, regulates proliferation and metastasis in breast cancer

So-Hyun Yoon

Cancer Biology

The Graduate School

Seoul National University

Background

Breast cancer is the most common cancer for women. Target genes are extracted based on Next generation sequencing (NGS) data for breast cancer patients to regulate their emergence and to study their function and mechanism in the formation and progression of cancer. In this study, we

studied NAD(P)-dependent steroid dehydrogenase-like (*NSDHL*), involved in cholesterol biosynthesis.

Methods

To detect *NSDHL* expression in breast cancer cells, we used SYBR™ Green Real-Time PCR, western blotting assay. To generate *NSDHL* knock-down cells, cells were transfected with siRNA using Lipofectamine 2000™. Cell proliferation assay, cell cycle analysis, 3D culture, clonogenic assay, migration assay, invasion assay, wound healing assay and total cholesterol assay of functional studies were performed. In addition, we identified erlotinib is efficient for treatment, as a target drug for *NSDHL*. Finally, we transfected shRNA of *NSDHL* in MDA-MB-231 and confirm *NSDHL* ability in NOD/SCID gamma mice. Clinically, we have performed Cox proportional hazard ratio model analysis for the effect of *NSDHL* expression on recurrence free survival (RFS) rates by using microarray gene expression data and clinical data deposited in Gene expression omnibus (GEO) database and also used in previous investigations.

Results

Both *NSDHL* mRNA and protein levels were highly expressed in luminal A breast cancer cell (MCF7) and triple negative breast cancer cells (MDA-MB-231, BT-20) than normal breast cancer cell (MCF10A). Silencing of *NSDHL* by siRNA decreased proliferation ($p< 0.01$), differentiation in breast cancer cells and sensitive at erlotinib. Also, *NSDHL* inhibited migration and invasion in triple negative breast cancer, especially in MDA-MB-231 cell ($p< 0.01$). Additionally, we found that *NSDHL* regulated total cholesterol levels. In *in vivo*, we observed that *NSDHL* regulated tumor progression ($p< 0.01$), metastasis and once again confirmed the function of *NSDHL*. And high *NSDHL* expression in a total of 3951 breast cancer patients could be associated with lower recurrence free survival and we found that *NSDHL* is a clinically meaningful gene.

Conclusions

In conclusion, we first identified the function of *NSDHL* gene in breast cancer to help the proliferation and metastasis of breast cancer cells and showed the possibility as a therapeutic target.

Key words: Breast cancer, *NSDHL*, Knock-down, Proliferation, Metastasis, Cholesterol, EGFR

Student Number: 2017 - 23758

Contents

List of Tables

List of Figures

List of Abbreviations

NSDHL; NAD(P)−dependent steroid dehydrogenase−like

ER; estrogen receptor

TNBC; triple negative breast cancer

HER−2; human epidermal growth factor 2

CI; confidential interval,

HR; hazard ratio

EGFR; epidermal growth factor receptor

ATCC; American Type Culture Collection

KCLB; Korean Cell Line Bank

FBS; fetal bovine serum

PBS; phosphate buffered saline

PCR; polymerase chain reaction

qRT−PCR; quantitative real−time polymerase chain reaction

mRNA; messenger RNA

siRNA; small interfering RNA

CDK2; Cyclin−dependent kinase 2

shRNA; short hairpin RNA

SREBP-1; Sterol regulatory element -binding transcription factor 1

LDLR; Low-density lipoprotein receptor

NSG mice; NOD/SCID gamma mice

H&E staining; Hematoxylin and eosin staining

Introduction

Breast cancer is common malignancy of women in Korea [1, 2] and the major cause of mortality in females worldwide [3]. Although various progress in early diagnosis, radiation therapy and various combination of surgery improved the prognosis of breast cancer patients [4], the high mortality rates are remained. Furthermore, the identification of novel therapeutic targets is important to discover the potential biomarkers for early diagnosis and prognosis in breast cancer patients.

In previous study, using whole exome sequencing in 120 breast tumor and normal paired tissues, they detected 11,684 putative somatic mutations in 7,373 genes. After selected 1,116 genes with 3 or more mutations, 695 genes were chosen using messenger RNA (mRNA) expression in the whole transcriptome sequencing data. Finally, 198 somatic mutations of 50 genes were selected in 64 patients. In this result, NAD(P)-dependent steroid dehydrogenase-like (*NSDHL*) has 3 mutations and high level of hazard ratios for recurrence using K-M plotter (Hazard Ratio = 1.43, 95% CI = 1.28 - 1.61, *P*-value < 0.001) [5].

NAD(P)-dependent steroid dehydrogenase-like is a protein coding gene. Also, localized in the endoplasmic reticulum and involved in cholesterol biosynthesis [6]. Obesity is considered important risk factor in cancer [7-10] but the cause is not elucidated. Oncogene-transformed cancer cells rapidly grow from elevated cholesterol levels. the cholesterol uptake process is regulated by epidermal growth factor receptor (EGFR) signaling [11-13]. *NSDHL*, catalyze oxidative decarboxylation of the C4 methyl group from MAS (Meiosis-activating sterols) [14, 15] has critical role to convert squalene to cholesterol [16] . Also, cholesterol is an essential component of the animal cell membranes [17]. *NSDHL* derived from ER membranes [18], translocated to the plasma membrane from the intracellular compartment by lipid-depleted serum (LDs) and cooperate with lipid rafts to promote metastasis [19-22]. *NSDHL* function in breast cancer has rarely been studied.

In the present study, in breast cancer cells, *NSDHL* expression of both mRNA and protein levels in MCF7, MDA-MB-231 and BT-20 cells were higher than non-tumorigenic epithelial cell (MCF10A). Among them, we inhibited *NSDHL* expression using small interfering RNA (siRNA) and

studied proliferation and migration potential in breast cancer cells related with EGFR and cholesterol pathway. Moreover, we found that *NSDHL* regulated total cholesterol levels. After then, the tumor growth and metastasis were confirmed in NOD/SCID gamma mice (NSG mice). Clinically, we identified Patients with high *NSDHL e*xpression in total of 3951 breast cancer patients showed unfavorable outcomes on recurrence free survival (RFS) rates. Taken together, these results demonstrated that *NSDHL* is pivotal for the tumorigenesis in breast cancer.

Materials and methods

1. *In vitro*

1) Breast cancer cell lines

Among the mutations confirmed by whole exome sequencing, we evaluated the function of *NSDHL*. The normal breast cancer cell line (MCF10A; by. Woo Hang Hur), luminal A (MCF7), luminal B (ZR-75-1, BT-474), HER2+ (SK-BR-3), triple negative breast cancer (TNBC) (BT-20, Hs578T, MDA-MB-231) were used in this study. MCF7, Hs578T and MDA-MB-231 cell lines were obtained from the American Type Culture Collection (ATCC), BT-20, BT-474, SK-BR-3 and ZR-75-1 cell lines were obtained from Korean Cell Line Bank (KCLB). MCF7, Hs578T and MDA-MB-231 cells were grown in DMEM (Welgene) supplemented with 10% fetal bovine serum (FBS; Welgene) and 1% Antibiotic-Antimycotic

(100X) (Gibco). BT-20, BT-474, SK-BR-3 and ZR-75-1 cells were grown in RPMI 1640 (Welgene) supplemented with 10% fetal bovine serum (FBS; Welgene) and 1% Antibiotic-Antimycotic (100X) (Gibco). All cells were maintained at 37℃ in a humidified atmosphere of 95% air with 5% CO2.

2) Primers, Antibodies and Drugs

For polymerase chain reaction (PCR), we used primers (GAPDH; F: GAGTCCAGGGCGTCTTCA, R: GGGGTGCTAAGCAGTTGGT), NSDHL; F: GGTGACGCACAGTGGAAAAC, R: TCGCACGGACTCATTTGACA). For western blot and immunohistochemistry, we used the following antibodies: β-actin (sc-47778), Sterol regulatory element -binding transcription factor 1 (SREBP-1) (sc-365513) from Santa Cruz; NSDHL (ab190353), EGFR (ab52894), Low-density lipoprotein receptor (LDLR) (ab52818) from Abcam; AKT (#9272), Cyclin-dependent kinase 2 (CDK2) (#2546) from Cell Signaling. For cell viability assay with drug

treatment, we used erlotinib HCl (OSl-744) (Selleckchem).

3) cDNA synthesis and quantitative Reverse Transcription- Polymerase Chain Reaction

Total RNA was extracted from cells using Tri-RNA Reagent (FAVORGEN). qRT-PCR reactions were conducted using cDNA kit (Applied Biosystems) and Power SYBR™ Green PCR Master Mix (Applied Biosystems). Reactions were performed by Real time PCR System (Light Cycler 480 Ⅱ, Roche) and the results were analyzed with the comparative Ct to establish relative expression curves.

4) Western Blotting and antibodies

Cells treated a concentration of 10 nM, 20 nM of siRNA were 48 h transfection. Total cell lysates prepared in lysis buffer (RIPA buffer, Phosphatase Inhibitor, 0.5M EDTA). Proteins concentrations were measured with the Pierce BCA Protein Assay Kit (Thermo scientific). Equal concentration of cell lysates was separated by 10% SDS PAGE. Immobilon - P Transfer Membranes (Merck Millipore L td) were blocked with blocking buffer (5% non-fat dry milk in TBS-T, 5% BSA in TBS-T) for 1 h. Primary antibodies were added to the blocking solution and incubates overnight at 4℃. Blots were washed three times (5 min, 5 min, 10 min) with TBS-T, and incubated with secondary antibodies for 1h at room temperature. After washing with TBS-T three times for 10 min each, immunocomplexes were visualized by chemiluminescence (Bio Molecular Imager, Amersham^{TM} Imager 600, GE Healthcare) with SuperSignal West Pico Chemiluminescent Substrate (Thermo scientific) and estimated molecular weight with Image J (National Institutes of Health).

5) siRNA transfection

The small interfering RNA targeting *NSDHL* and control Non-targeting pool were obtained from Dharmacon (Dharmacon Inc., Lafayette, CO). Transient transfection of cells was performed using Lipofectamine 2000 RNAiMAX Reagent (Invitrogen; Thermo Fisher Scientific, Inc.). Further experiments performed after. The *NSDHL* siRNA sequence was: GAGGAUAUGCUGUCAAUGU and Non-targeting pool sequence was: UGGUUUACAUGUCGACUAA.

6) Cell proliferation assay

A concentration of 20 nM of siRNA, 48 h transfected cells were evaluated by CellTiter-Glo® Luminescent Cell Viability Assay Kit (Promega) as described in 96 h. Cells were plated at 3,000 cells/100 μl in triplicate in 96-well plate incubated at 37℃. CellTiter-Glo assay buffer was added

100 μl (1:1) and measured by Luminescence (Luminoskan Ascent® Microplate Luminometers, Thermo scientific).

7) Cell cycle analysis

Treated $1x10^6$ cells were fixed in 700 μl 70% cold ethanol included in 300 μl phosphate buffered saline (PBS) and leave it in overnight, 4℃. Before analyzed, washed the cells twice in cold PBS and added 250 μl of PBS included 5 μl of 10 mg/ml of Rnase A (0.5 mg/ml) at 37℃ for 1 h. Keep in 4℃ after added 10 μl of 1 mg/ml propidium iodide (10 μg/ml, PI; Sigma). Cell cycle analysis was performed using the ModFit 3.0 (#441622, Verity software House)

8) Three-dimensional Matrigel culture (Sphere formation)

Cell imaging coverglass, 8 chambers (Eppendorf) were coated with matrigel (BD Biosciences) at 8 mg/ml in 250 μl and incubated at 37℃ for 4 h. Extracted cells ($1x10^5$ cells/ml) were diluted with 0.5 mg/ml Matrigel and spread on the 8 mg/ml Matrigel (1:1) then incubated at 37℃. Observed chambers for 9 day under a microscope (x40) (Leica DM IL LED, Leica Microsystems). And we measured sphere surface area formation ($A = \pi r^2$)

9) Colony formation assay

Single cell suspensions of cells were thoroughly suspended and single cells plated at $1.5x10^3$ cells/ml in full media in 6-well plate. After 9 day, to confirmed the efficiently cell-clusters, we determined microscopically (x40) (Leica DM IL LED, Leica Microsystems) and measured colony surface area (μm). After then, fixed with 4% formaldehyde for 30 min and

stained with 0.1% crystal violet. For measured the concentration of staining cells, washed the stained crystal violet with 400 μl of 10% acetic acid and read in (SpectraMax 190 Microplate Reader, Molecular Devices) (Lm: 570).

10) Drug treatment assay

The effect of erlotinib on transfected in MCF7, MDA-MB-231, BT-20 cells were measured using CellTiter-Glo Assay Kit (Promega) and measured by Luminescence (Luminoskan Ascent® Microplate Luminometers, Thermo scientific). Corresponding dilutions of DMSO were added as vehicle. Cells were plated at 3,000 cells/100 μl in triplicate in 96-well plate incubated at 37℃. After 24 h, the complete medium was replaced with various doses (0 μm - 160 μm) of vehicles and incubated at 37℃ during 72 h.

11) Transwell migration assay

Cells transfected with 20 nM of siRNAs for 48 h were seeded in the upper transwell chambers (8.0 μm pores sized) at a density of $5x10^4$ cells in 200 μl serum-free medium. Filled with 750 μl full DMEM containing 10% FBS and 1% Antibiotic-Antimycotic. After incubated for 24 h at 37℃, fixed chambers with 400 μl of 4% paraformaldehyde for 30 min and stained with 400 μl of 0.1% crystal violet for 30 min. Washed with distilled water and cleaned upper chamber with a cotton swab. Drying chambers then photographed (x40) (Leica DM IL LED, Leica Microsystems). For measured the concentration of staining cells, washed the stained crystal violet with 400 μl of 10% acetic acid and read in (SpectraMax 190 Microplate Reader, Molecular Devices) (Lm: 570).

12) Invasion assay

Cells transfected with 20 nM of siRNAs for 48 h were seeded in the upper transwell chambers (8.0 μm pores sized) coated with 100 μl of 1 mg/ml matrigel (BD Biosciences) before 4 h performed assay. Added a density of $5x10^4$ cells in 100 μl serum−free medium (1:1) on the matrigel. Filled with 750 μl full DMEM containing 10% FBS and 1% Antibiotic−Antimycotic. After incubated for 24 h at 37℃, fixed chambers with 400 μl of 4% paraformaldehyde for 30 min and stained with 400 μl of 0.1% crystal violet for 30 min. Washed with distilled water and cleaned upper chamber with a cotton swab. Drying chambers then photographed (x40) (Leica DM IL LED, Leica Microsystems). For measured the concentration of staining cells, washed the stained crystal violet with 400 μl of 10% acetic acid and read in (SpectraMax 190 Microplate Reader, Molecular Devices) (Lm: 570).

13) Wound healing assay

$4x10^5$ cells/500 μl transfected with siRNAs were seeded in 24-well plate in triplicate and incubated at 37℃ for overnight. After cells were full, using 1000 μl pipette tips made a straight scratch and washed in PBS. Then filled with 500 μl of full media. Observed at intervals of 24 h from 0 h to 24 h (x40) (Leica DM IL LED, Leica Microsystems).

14) Total cholesterol assay

Cells treated a concentration of 20 nM of siRNA were seeded for 48 h transfection. For $1x10^6$ cells, extracted with 200 μl of a mixture of chloroform : isopropanol : tritonx-100 (7:11:0.1) and centrifuge (10 min, 15,000 rcf, 25℃). Transfered the liquid to a new e-tube, then air dry at 50℃. Put samples under vacuum (30 min) (SPD1010 & SPD2010, Thermo scientific). 200 μl of 1X Assay buffer (Total cholesterol Assay Kit

(Fluorometric), STA-390) was added in dried lipids and vortexed. After solutions were homogenous and cloudy, measured 50 μl per well in triplicate with cholesterol reaction reagent (diluting the Cholesterol Oxidase 1:50, HRP 1:50, Fluorescence Probe 1:50, and Cholesterol Esterase 1:250 in 1X Assay Diluent. Determine the cholesterol concentration of the samples with the equation obtained from the linear regression analysis of the standard curve.

Total Cholesterol (μm) = Sample corrected absorbance / Slope x Sample dilution,

2. *In vivo*

1) shRNA lentiviral particle transduction

Plated $4x10^5$ MDA-MB-231 cells in 12-well plate 24 h prior to viral infection. Replace with 1 ml of 5 μg/ml Polybrene® (sc-134220) media mixture and 20 μl of control shRNA Lentiviral Particles-A (sc-108080), *NSDHL* shRNA (h) Lentiviral Particles (sc-90849-V). After 24 h, replaced with 1 ml of full media and incubated overnight. Split cells 1:5 and continue incubated for 48 h in full media. Change with 10 μg/ml Puromycin dihydrochloride (sc-108071) of full media for 7 day.

2) NOD.Cg-Prkdc^{scid} Il2rg^{tm1wjl}/SzJ mice

NOD/SCID gamma mice obtained from The Jackson Laboratory were approved by the Institutional Animal Care and Use Committee (IACUC).

NSG mice born between july 31, 2018 and august 9, 2018 were tested on september 21, 2018. 5 shCONTROL mice and 5 shNSDHL mice were injected 100 μl of $1x10^6$ cells with cold 1X PBS and 10 mg/ml matrigel (BD Biosciences, Franklin Lakes, NJ, USA) (1:1) into each left breast. We calculated tumor volume using formation.

(V (Tumor Volume) = L (Length) x W (Width) x W / 2)

2) Immunohistochemistry

Blocks of paraffin-embedded tissue from NSG mice were cut in serial 4-μm sections and lung tissues were stained for H&E from pathology lab. Tumor tissues were incubated in dry oven (60℃) and deparaffinized in xylene. After 20 min, we rehydrated through ethanol and microwaved in 1X Antigen retrieval solution (S1699, Dako). For blocking tissues, Immuno blocking solution with goat serum (AR-6591-02, Immuno bioscience) was added and incubated in 4℃. On the slides, diluted 1st antibody NSDHL(1:100, ab190353, Abcam) with Dako antibody diluent with

background reducing components (S3022, Dako) at 4℃ for overnight. The immunoreactions were detected using DAB kit (K5007, Dako) and stained with hematoxylin and Mayer's (S330930-2, Dako). After staining, we performed dehydration and determined microscopically (x100) (Light Microscope with imaging system, iSolution Lite, Image & Microscope Technology).

3. Clinical Prognostic Implication of *NSDHL* Expression level in Survival of Breast Cancer Patients

We have performed Cox proportional hazard ratio model analysis for the effect of *NSDHL* expression on recurrence free survival (RFS) rates of a total of 3951 breast cancer patients (including cases with luminal A (n=1933), luminal B (n=1149), HER2−positive (n=252), HER2−negative (n=800), Basal (n=618), ER−positive (n=3083), ER−negative (n=873), and TNBC (n=198) subtypes) by using microarray gene expression data and clinical data deposited in Gene expression omnibus (GEO) database and also used in previous investigations [5].

4. Statistics

Each experiment was done in triplicate. Statistical analyses were calculated by using Student's t Test (*: $p<0.05$, **: $p<0.01$) (GraphPad Prism v6.01 software for Windows).

Results

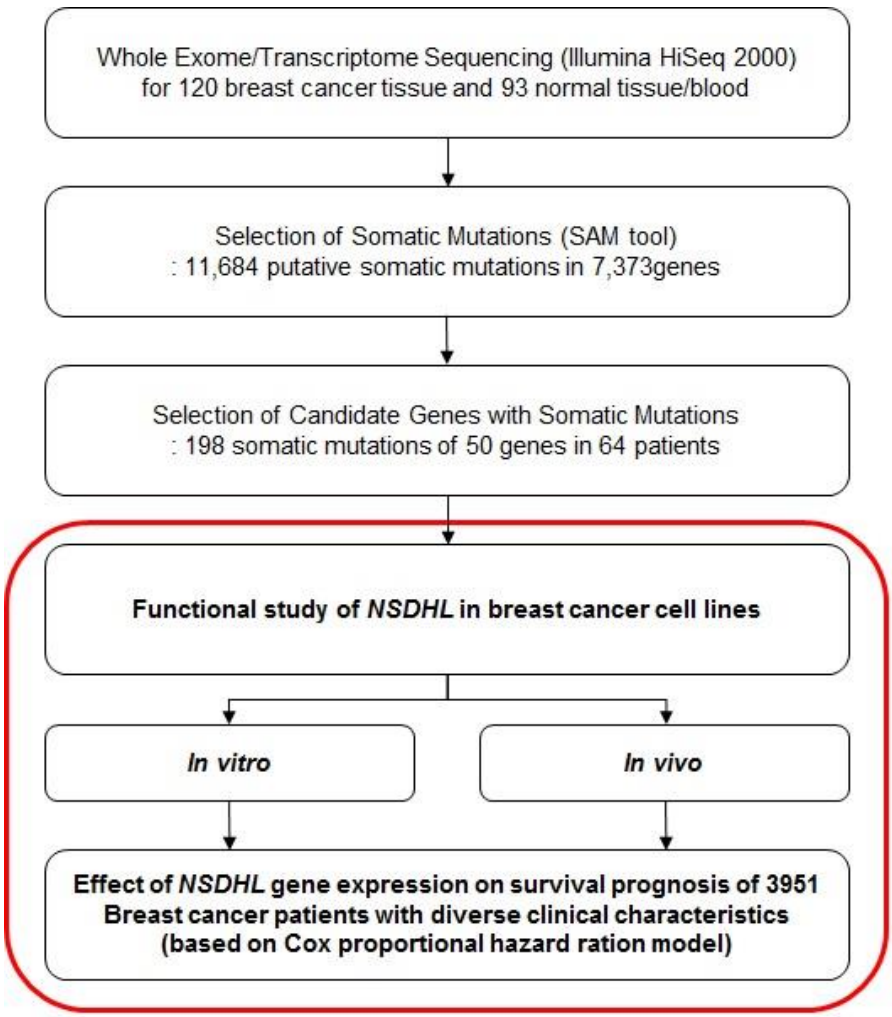

Figure 1. Scheme of this study

Table 1. 198 somatic mutations of 50 genes in 64 patients through whole exome sequencing of 120 breast cancers [5]

Gene	Description	Position	R_ base	A_ base	No. of mutation
NSDHL	NAD(P)−dependent steroid	X:152018879	G	C	1
	dehydrogenase−like	X:152027402	G	A	1
		X:152037444	C	A	1

Table 2. Hazard ratios for recurrence of *NSDHL* in 3951 breast cancer patients using Cox proportional hazard ratio model analysis

Genes	Total (N=3951)			luminal A (N=1933)			luminal B (N=1149)			HER-2 positive (N=252)			Basal (N=618)		
	HR	CI	*P*	HR	CI	*P*	HR	CI	*P*	HR	CI	*P*	HR	CI	*P*
NSDHL	1.419	1.267-1.59	<0.001	1.307	1.103-1.55	0.00197	1.372	1.119-1.684	0.002313	0.8341	0.56-1.242	0.3715	1.37	1.054-1.779	0.001806

Table 3. Univariate and multivariable analysis by *NSDHL*

Characteristics		Univariate analysis			Multivariable analysis		
		HR	95% CI	*P*	HR	95% CI	*P*
Tumor Grade	I	**1.814**	1.077−3.055	0.02319			
	II	**1.365**	1.066−1.748	0.0132			
	III	0.774	0.6212−0.9654	0.02264			
Subtypes	Basal	**2 (ref)**			**1.2703**	1.1414−1.4137	3.975×10^{-7}
	luminal A	**2 (ref)**					
	luminal B	**2 (ref)**					
	TNBC	**1.605**	0.9134−2.819	0.09691			
	HER2−Positive	**2 (ref)**					
Lymph Node	Positive	**1.253**	1.044−1.503	0.0153	**1.328**	1.156−1.527	0
	Negative	**1.425**	1.149−1.768	0.00118			
Estrogen receptor	Positive	**1.372**	1.195−1.574	6.234×10^{-6}	**1.344**	1.1949−1.5117	0
	Negative	**1.287**	1.026−1.613	0.02844			
Progesterone Receptor	Positive	**2.034**	1.426−2.903	6.42×10^{-5}	**1.543**	1.2239−1.9445	7.246×10^{-11}
	Negative	1.277	0.9419−1.731	0.1145			
HER−2	Positive	0.5789	0.3648−0.9187	0.01884	**1.199**	0.9252−1.555	0.08981
	Negative	**1.531**	1.157−2.027	0.002674			
TP53	Wild Type	**1.66**	1.037−2.658	0.03281	**1.712**	1.211−2.421	0.0003498
	Mutant Type	**1.735**	1.05−2.867	0.02948			

1. *In vitro*

1) Expression of *NSDHL* in breast cancer cell lines

In order to identify the function of *NSDHL*, the *NSDHL* mRNA and protein levels were detected in 8 breast cancer cell lines (MCF10A, MCF7, ZR-75-1, BT-474, SK-BR-3, BT-20, Hs578T, MDA-MB-231) (Figure 2A, B and C). Based on *NSDHL* mRNA and protein expressions, we were selected MCF7, MDA-MB-231 and BT-20 cells highly expressed in both mRNA and protein levels than MCF10A cell. By transfection of *NSDHL* siRNA, *NSDHL* was knocked down in these cells ($p<0.01$). The mRNA level (Figure 3A and B) and protein expressions (Figure 3C) were downregulated by *NSDHL* siRNA in these cell lines. *NSDHL* expression is significantly decreased in breast cancer cell lines at 48 h after transfection with scramble siRNA. These results suggested that suppression of *NSDHL* lead the inhibition of breast cancer cell lines.

A

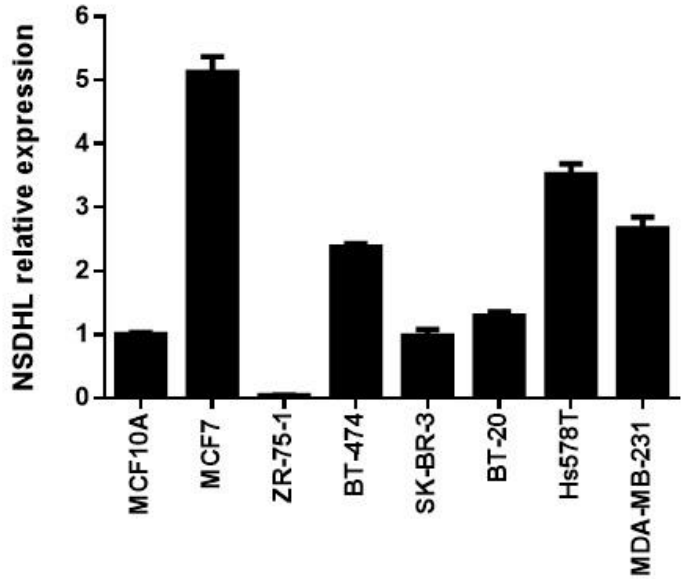
NSDHL relative expression
6
5
4
3
2
1
0
MCF10A
MCF7
ZR-75-1
BT-474
SK-BR-3
BT-20
Hs578T
MDA-MB-231

B

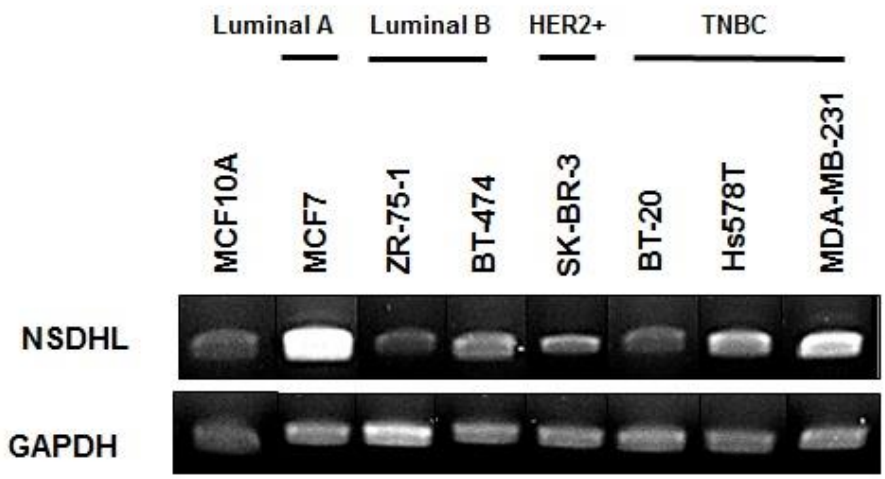
Luminal A
Luminal B
HER2+
TNBC
MCF10A
MCF7
ZR-75-1
BT-474
SK-BR-3
BT-20
Hs578T
MDA-MB-231
NSDHL
GAPDH

C

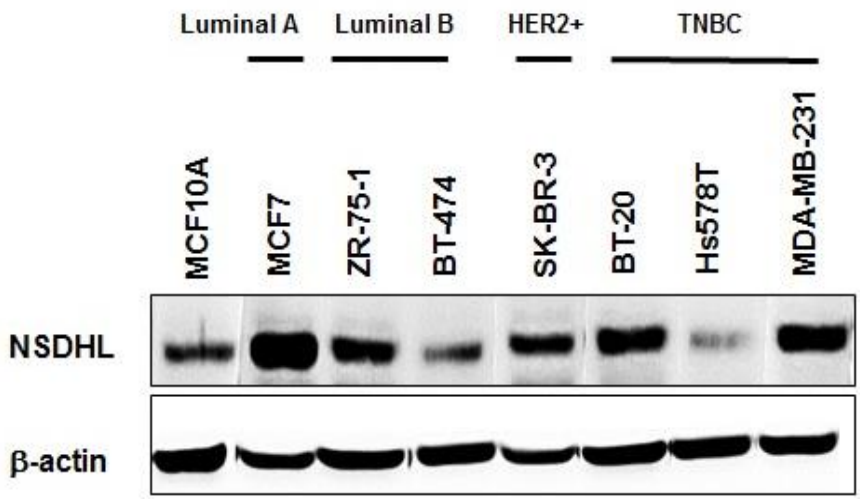

Figure 2. *NSDHL* expression in 8 breast cancer cell lines in (A) RT-qPCR (B) PCR and (C) western blot analysis.

A

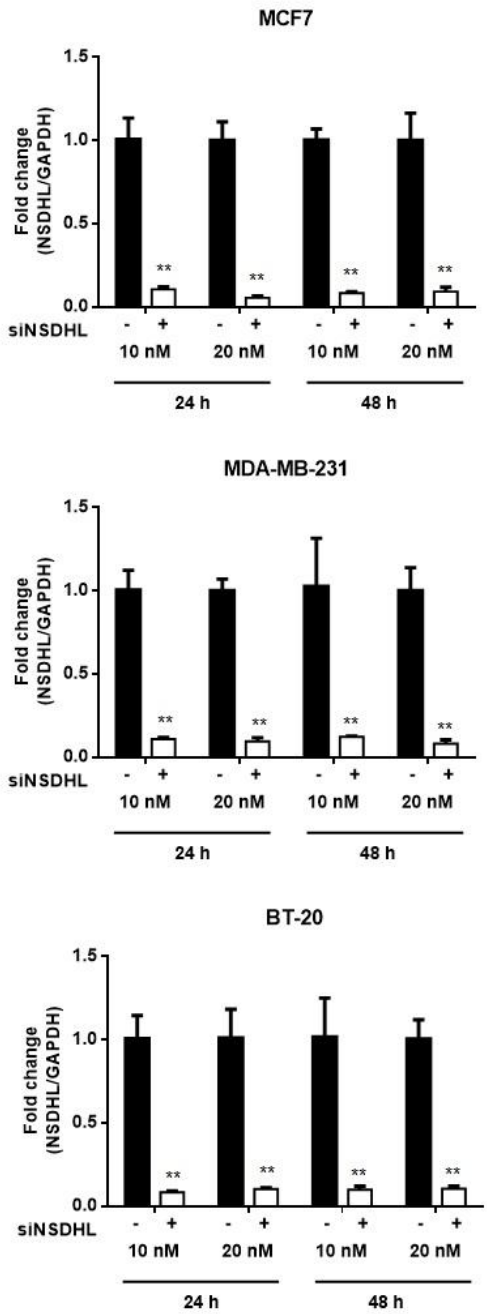
MCF7
Fold change (NSDHL/GAPDH)
1.5
1.0
0.5
0.0
**
siNSDHL
- + - + - + - +
10 nM 20 nM 10 nM 20 nM
24 h 48 h
MDA-MB-231
BT-20

B

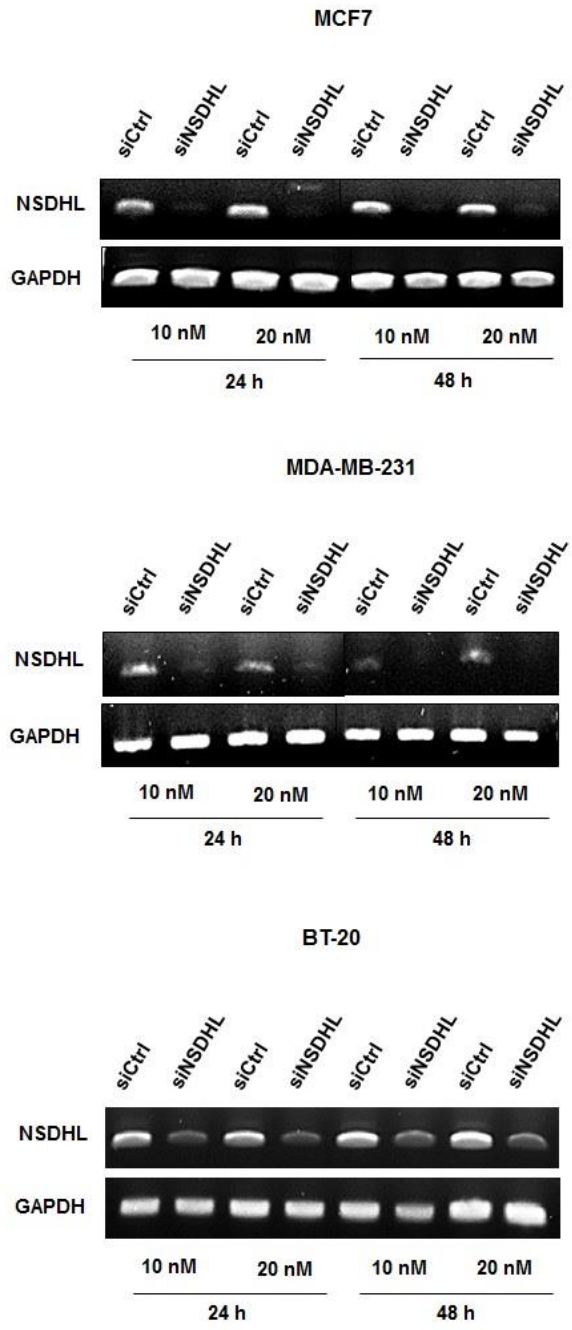
MCF7
siCtrl
siNSDHL
siCtrl
siNSDHL
siCtrl
siNSDHL
siCtrl
siNSDHL
NSDHL
GAPDH
10 nM
20 nM
10 nM
20 nM
24 h
48 h
MDA-MB-231
siCtrl
siNSDHL
siCtrl
siNSDHL
siCtrl
siNSDHL
siCtrl
siNSDHL
NSDHL
GAPDH
10 nM
20 nM
10 nM
20 nM
24 h
48 h
BT-20
siCtrl
siNSDHL
siCtrl
siNSDHL
siCtrl
siNSDHL
siCtrl
siNSDHL
NSDHL
GAPDH
10 nM
20 nM
10 nM
20 nM
24 h
48 h

C

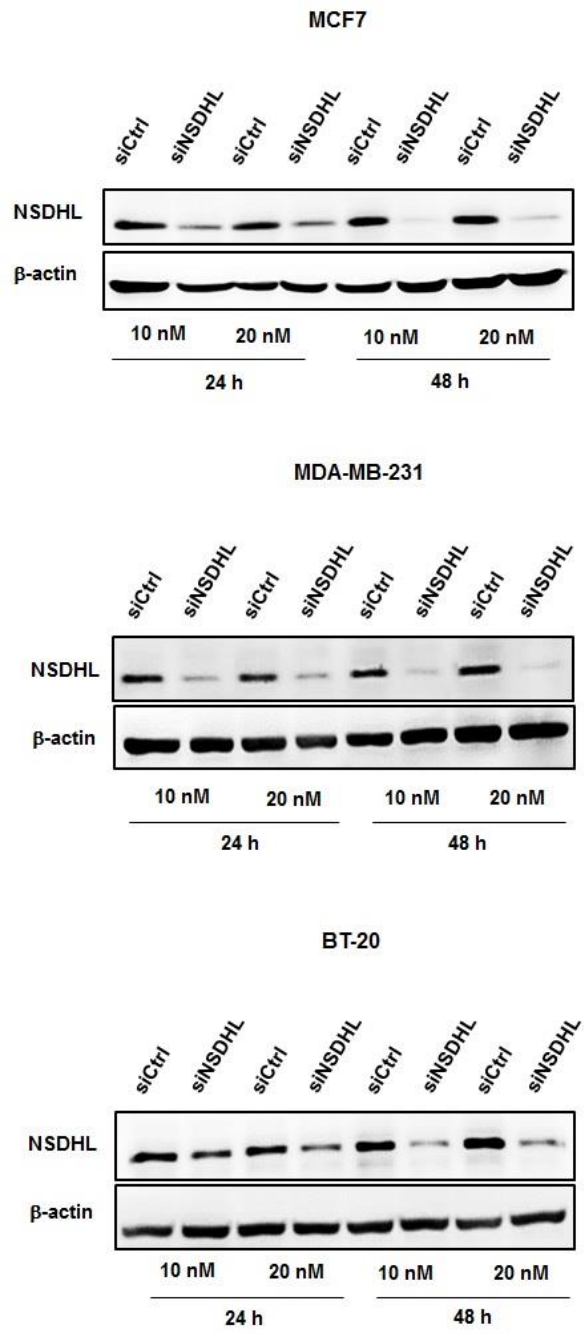
MCF7
siCtrl
siNSDHL
siCtrl
siNSDHL
siCtrl
siNSDHL
siCtrl
siNSDHL
NSDHL
β-actin
10 nM
20 nM
10 nM
20 nM
24 h
48 h
MDA-MB-231
siCtrl
siNSDHL
siCtrl
siNSDHL
siCtrl
siNSDHL
siCtrl
siNSDHL
NSDHL
β-actin
10 nM
20 nM
10 nM
20 nM
24 h
48 h
BT-20
siCtrl
siNSDHL
siCtrl
siNSDHL
siCtrl
siNSDHL
siCtrl
siNSDHL
NSDHL
β-actin
10 nM
20 nM
10 nM
20 nM
24 h
48 h

Figure 3. Downregulation of *NSDHL* expression in MCF7, MDA-MB-231 and BT-20 cells by siRNA transfection. (A), (B) Relative expression levels of *NSDHL* mRNA level of *NSDHL* knock-down MCF7, MDA-MB-231 and BT-20 cells were detected by RT-qPCR. (C) Expression of *NSDHL* proteins was detected by western blot assay. These results demonstrated that *NSDHL* expressed in MCF7, MDA-MB-231 and BT-20 cells. Therefore, *NSDHL* siRNA remarkably inhibited the expression of *NSDHL* mRNA and proteins level in breast cancer cells. Each value was expressed as mean ± S.D. Each experiment was done in triplicate. * $p<0.005$; ** $p<0.001$ (Multiple t-test).

2) Silencing of *NSDHL* inhibits the proliferation of MCF7, MDA-MB-231 and BT-20 cells

To determine the effect of *NSDHL* on cell growth, cell viability by Cell-titer glo assay kit, 3D culture assay, colony formation assay and cell cycle assay were performed after inhibited with siRNA. Compared with the control cells, after 48 h treated 20 nM *NSDHL* siRNA transfected cell's (Figure 4B) growth curves showed significantly lower for 96 h of incubation measured by cell viability assay, especially in MDA-MB-231 cells (Figure 4A). Moreover, 3D sphere formation showed that the treated siNSDHL cells slowly differentiated for 9 day than control cells (Figure 4C). Correlated with colony formation, control cell significantly grown than siNSDHL transfected cells (Figure 4D, E). Also, Silencing of *NSDHL* inhibited the cell cycle than transfected with the siCONTROL (Figure 4F). After 48 h transfection with *NSDHL* siRNA in MCF7 and MDA-MB-231 cells, the percentage of cells in S and G2/M phases was decreased ($p<0.01$), but not in BT-20 cell. In BT-20 cell, G0/G1 phase was decreased ($p<0.05$). To support these results, we found that EGFR, CDK2

and LDLR expressions were inhibited in siRNA transfected cells (Figure 8B). These results indicated that *NSDHL* siRNA regulated the MCF7, MDA-MB-231 and BT-20 in cell cycle, delayed the progression of cell cycle and lead to inhibition of cell proliferation.

A

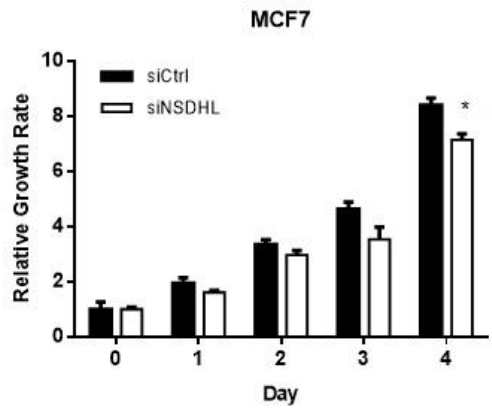
MCF7
siCtrl
siNSDHL
Relative Growth Rate
Day
*

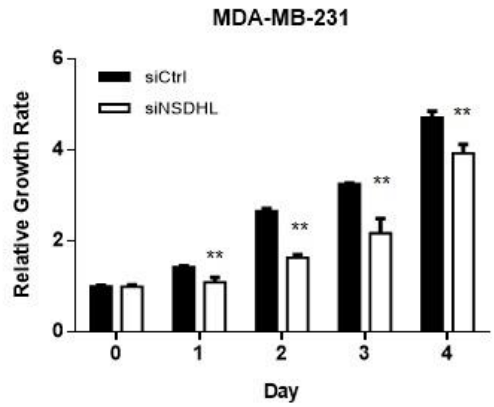
MDA-MB-231
siCtrl
siNSDHL
Relative Growth Rate
Day
**

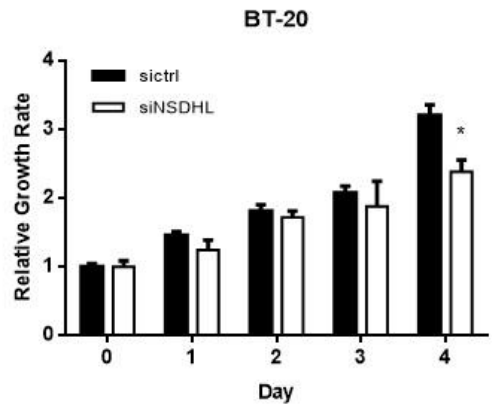
BT-20
sictrl
siNSDHL
Relative Growth Rate
Day
*

B

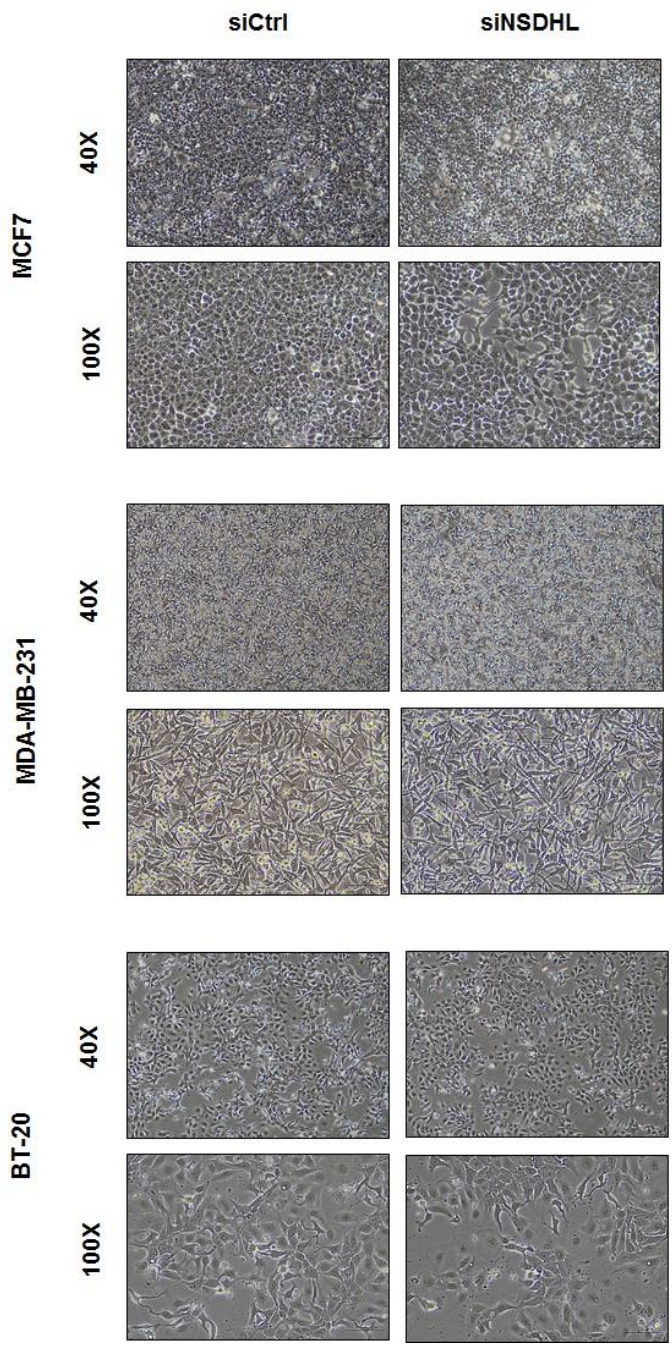
siCtrl
siNSDHL
MCF7
40X
100X
MDA-MB-231
40X
100X
BT-20
40X
100X

C

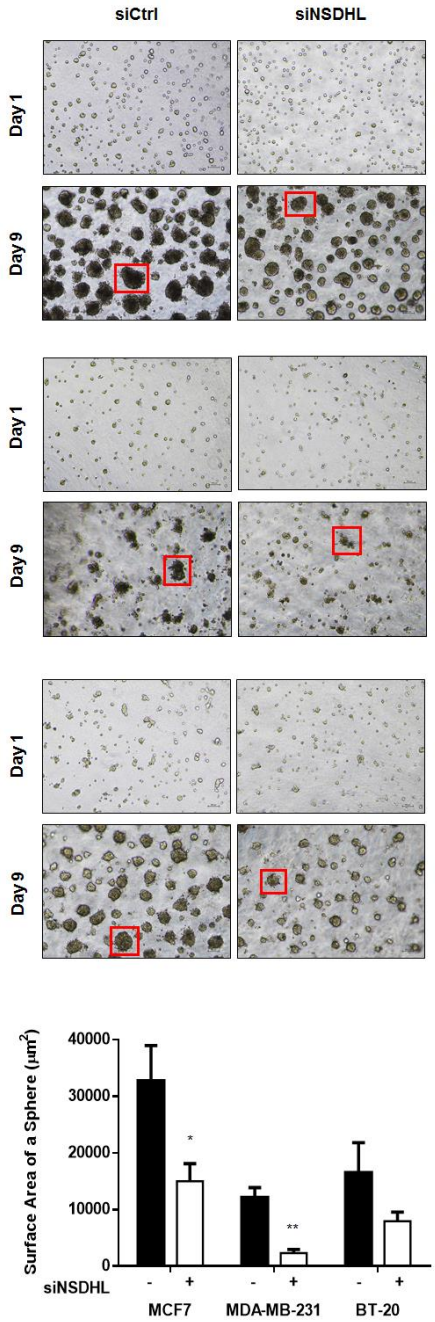
siCtrl
siNSDHL
Day 1
Day 9
Day 1
Day 9
Day 1
Day 9
Surface Area of a Sphere (μm²)
40000
30000
20000
10000
0
*
**
siNSDHL
-
+
-
+
-
+
MCF7
MDA-MB-231
BT-20

D

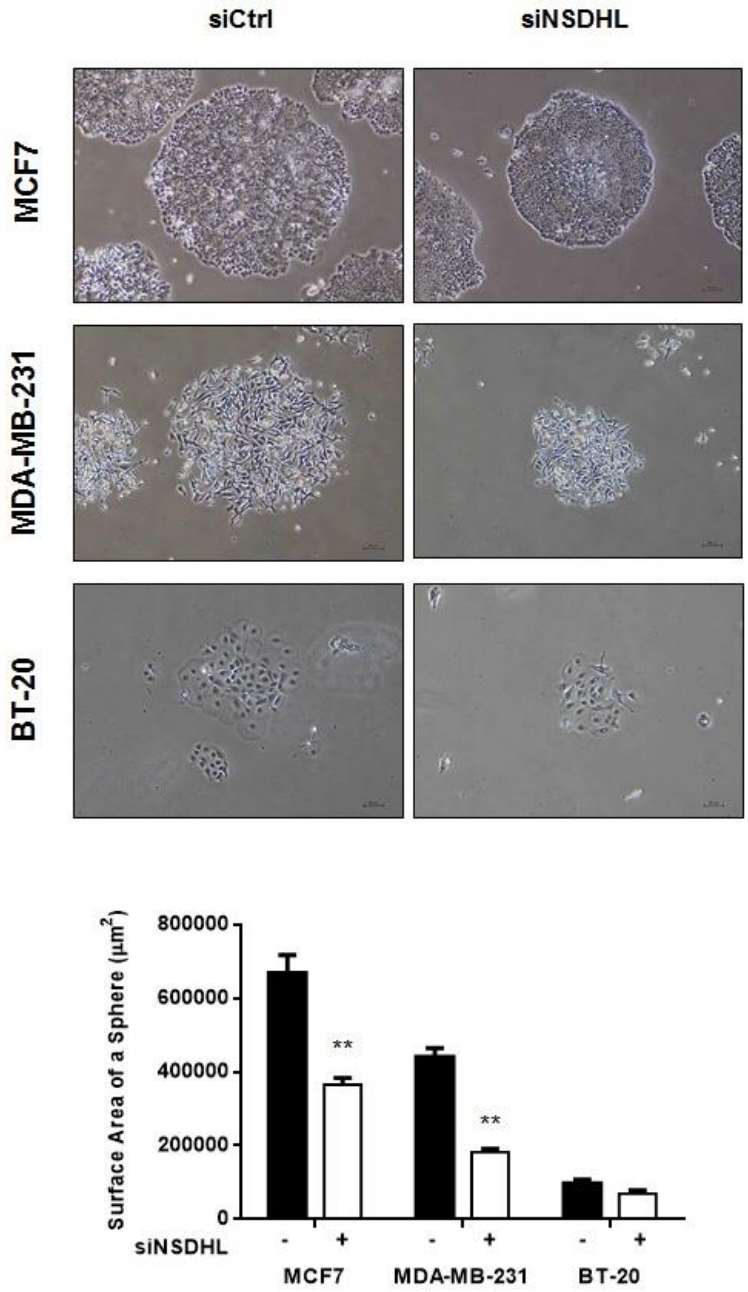
siCtrl
siNSDHL
MCF7
MDA-MB-231
BT-20
Surface Area of a Sphere (μm²)
800000
600000
400000
200000
0
**
**
siNSDHL
-
+
-
+
-
+
MCF7
MDA-MB-231
BT-20

E

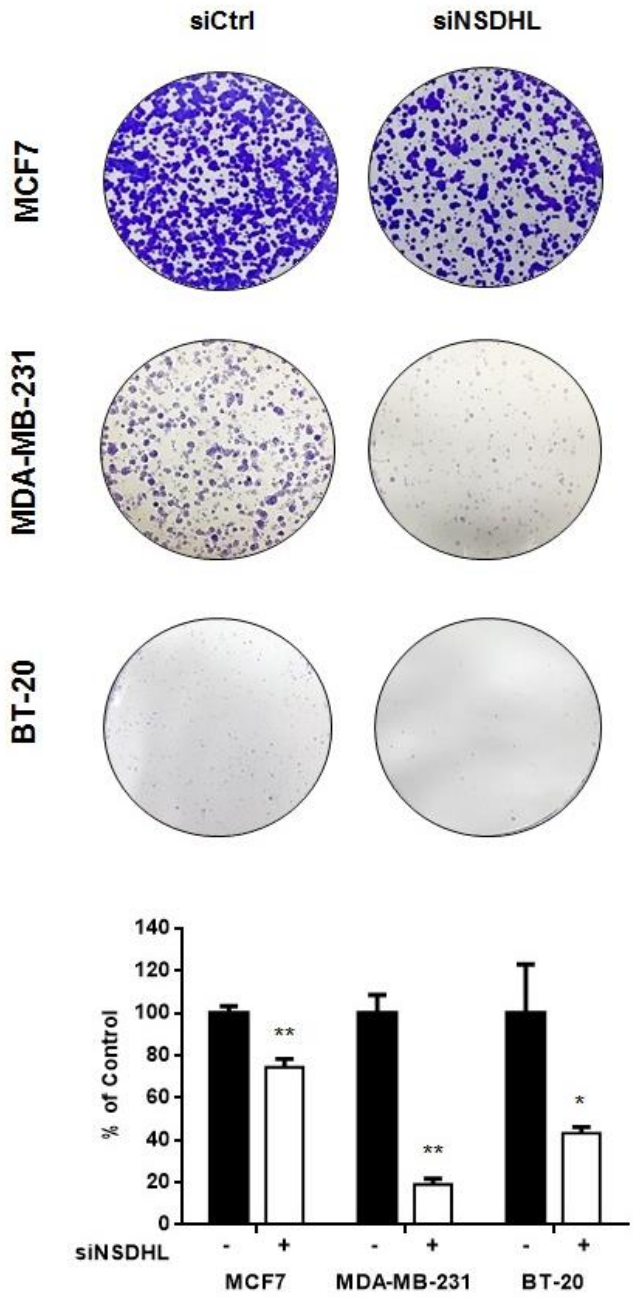
siCtrl
siNSDHL
MCF7
MDA-MB-231
BT-20
% of Control
140
120
100
80
60
40
20
0
**
**
*
siNSDHL
-
+
-
+
-
+
MCF7
MDA-MB-231
BT-20

F

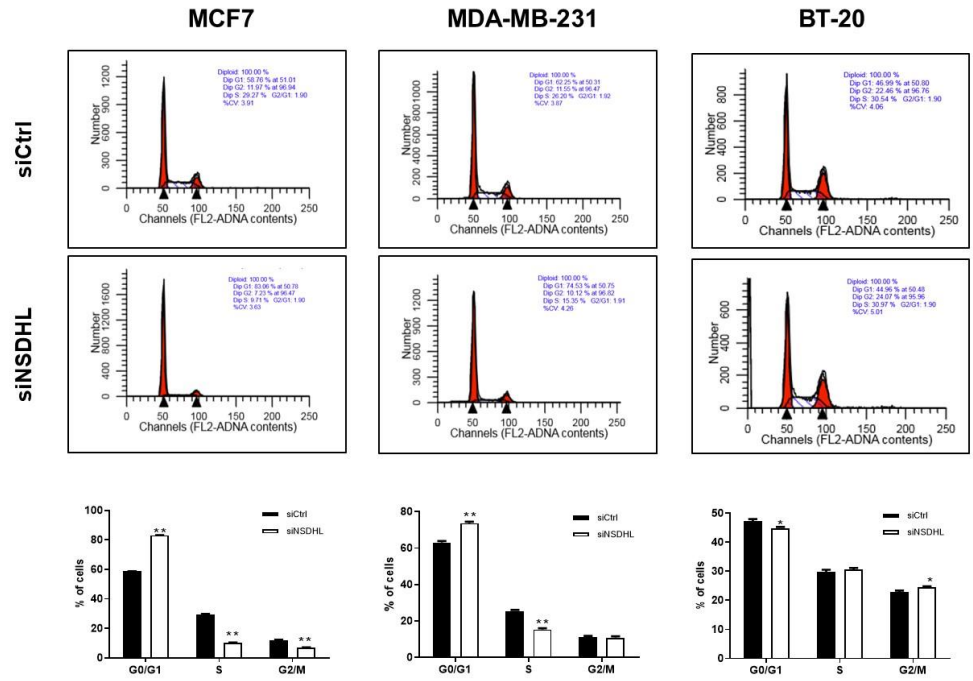
MCF7
MDA-MB-231
BT-20
siCtrl
siNSDHL
Number
Channels (FL2-ADNA contents)
% of cells
siCtrl
siNSDHL
G0/G1
S
G2/M

Figure 4. Knock-down of *NSDHL* inhibited breast cancer cells proliferation. (A) Cell viability of *NSDHL* in cells treated with siRNA 20 nM, 48 h post transfection) for 96 h. These data showed cell growth inhibition by silencing of *NSDHL* treatment. Treated siNSDHL in MDA-MB-231 cell were more effectively reduced than MCF7 and BT-20 cells. (B) 2D culture (x40) and (C) 3D culture assay (x40), coated with matrigel indicated that reduction of proliferation in siNSDHL transfection cells for 9 day. Correlated with colony formation, (D) colony area and (E) concentration of stained control cells significantly more than siNSDHL transfected cells. (F) *NSDHL* function in cell cycle, in these data showed that cells treated siNSDHL, increased in G0/G1 phase of MCF7, MDA-MB-231 cells but S and G2/M phases in BT-20 cell. These data demonstrated that cell proliferation was significantly inhibited by siNSDHL treatment in breast cancer cells. Data were expressed as mean ± standard deviation. Each experiment was done in triplicate. * $p<0.005$; ** $p<0.001$ (Multiple t-test).

3) Effect of erlotinib in silencing of *NSDHL* in MCF7, MDA-MB-231 and BT-20 cells

Erlotinib is an epidermal growth factor receptor tyrosine kinase inhibitor. It inhibits EGF-dependent cell proliferation and blocks cell-cycle progression in the G1 phase. To identify the function of *NSDHL* and erlotinib in cell growth, we evaluated IC50 concentration, treated 20 nM after 48 h cells for 72 h incubation. The IC50 value was the range of 0 μm – 160 μm and detected by Luminescence using CellTiter-Glo® Luminescent Cell Viability Assay Kit (Promega). In Table 4 and Figure 5A, B, and C, erlotinib could inhibit cell proliferation in a dose-dependent manner. In detail, the IC50 value in MCF (– 74.07, + 46.42), MDA-MB-231 (– 83.54, + 27.62) and BT-20 (– 168.2, + 78.28) cells. Furthermore, the highest sensitivity was found in siCONTROL of BT-20 cell (Figure 5C) and the difference between siCONTROL and siNSDHL was largest in MDA-MB-231 cell (Figure 5B). The sensitivity of erlotinib was significantly lower in siNSDHL treated cells, especially in MDA-MB-231 (p<0.01). Also, the extent of proliferation is consistent with the degree

of knock-down levels in protein of EGFR and CDK2 (Figure 8B). In these results indicated that erlotinib effectively reduced transfected *NSDHL* siRNA in breast cancer cells in relative to EGFR pathway.

Table 4. IC_{50} of erlotinib in silencing of siCONTROL (−) and siNSDHL (+) in breast cancer cells

Cell lines	Drug name	IC_{50}(μM)
MCF7 −	erlotinib	74.07
MCF7 +	erlotinib	46.42
MDA−MB−231 −	erlotinib	83.54
MDA−MB−231 +	erlotinib	27.62
BT−20 −	erlotinib	168.2
BT−20 +	erlotinib	78.28

A

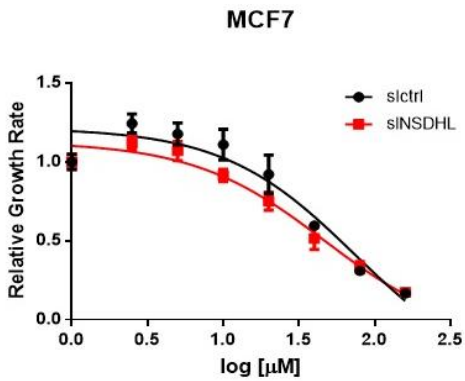
MCF7
sictrl
siNSDHL
Relative Growth Rate
log [μM]

B

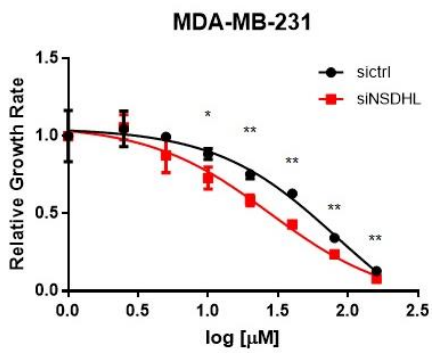
MDA-MB-231
sictrl
siNSDHL
Relative Growth Rate
log [μM]

C

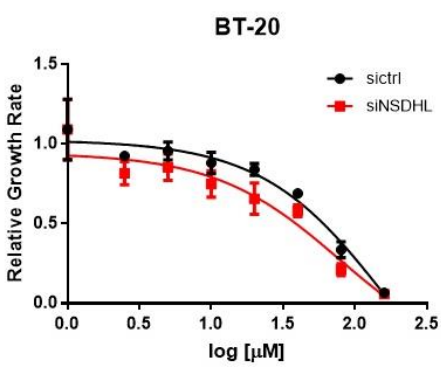
BT-20
sictrl
siNSDHL
Relative Growth Rate
log [μM]

Figure 5. EGFR inhibitor reduces cell sensitivity in silencing of *NSDHL* in breast cancer cells. Erlotinib could inhibit cell proliferation in a dose-dependent manner. Control and siRNA transfection cells were treated with erlotinib in concentrations ranging to 0 to 160 μM at 72 h and determined by Cell Titer-Glo® assay. As shown in (A), (B), (C), the sensitivity of erlotinib on knock-down cells were decreased. In detail, the IC50 value in MCF (− 74.07, + 46.42), MDA-MB-231 (− 83.54, + 27.62) and BT-20 (− 168.2, + 78.28) cells. Given that erlotinib is reduced cell viability. These results indicated that EGFR pathway is affected by MCF7, MDA-MB-231 and BT-20 cells in relation to *NSDHL*. Data were expressed as mean ± standard deviation. Each experiment was done in triplicate. * $p<0.005$; ** $p<0.001$ (Multiple t-test).

4) Downregulation of *NSDHL* inhibits MDA-MB-231 and BT-20 cells in the migration and Invasion

Since cancer cell migration play very critical roles in cancer metastasis, we investigated the effect of *NSDHL* suppression on transwell, invasion and wound healing assays. After 48 h, treated 20 nM *NSDHL* siRNA cells demonstrated reduction, especially in MDA-MB-231 cell. The transwell assay revealed that the loss of *NSDHL* expression could significantly decrease the migration rate by 60% in MDA-MB-231 cell, 30% in BT-20 cells comparison with scrambled siRNA-treated cells (Figure 6A). Results from invasion assay supported these data, reduced by 53% in MDA-MB-231 cells and 10% in BT-20 cells (Figure 6B). Consistently, the wound healing assay also showed that the migration rate was decreased by silencing of *NSDHL* in TNBC cells (Figure 6C). In detail, compared with the control cell groups, scratch wound reduced differently for 24 h, especially in MDA-MB-231 cells ($p<0.05$). In western blotting assay, we found that binding to specific sterol element, SREBP-1 and LDLR expressions were reduced in siRNA transfected cells (Figure 8B).

Therefore, these data indicated that the pivotal role of *NSDHL* on the migration and invasion in TNBC cells.

A

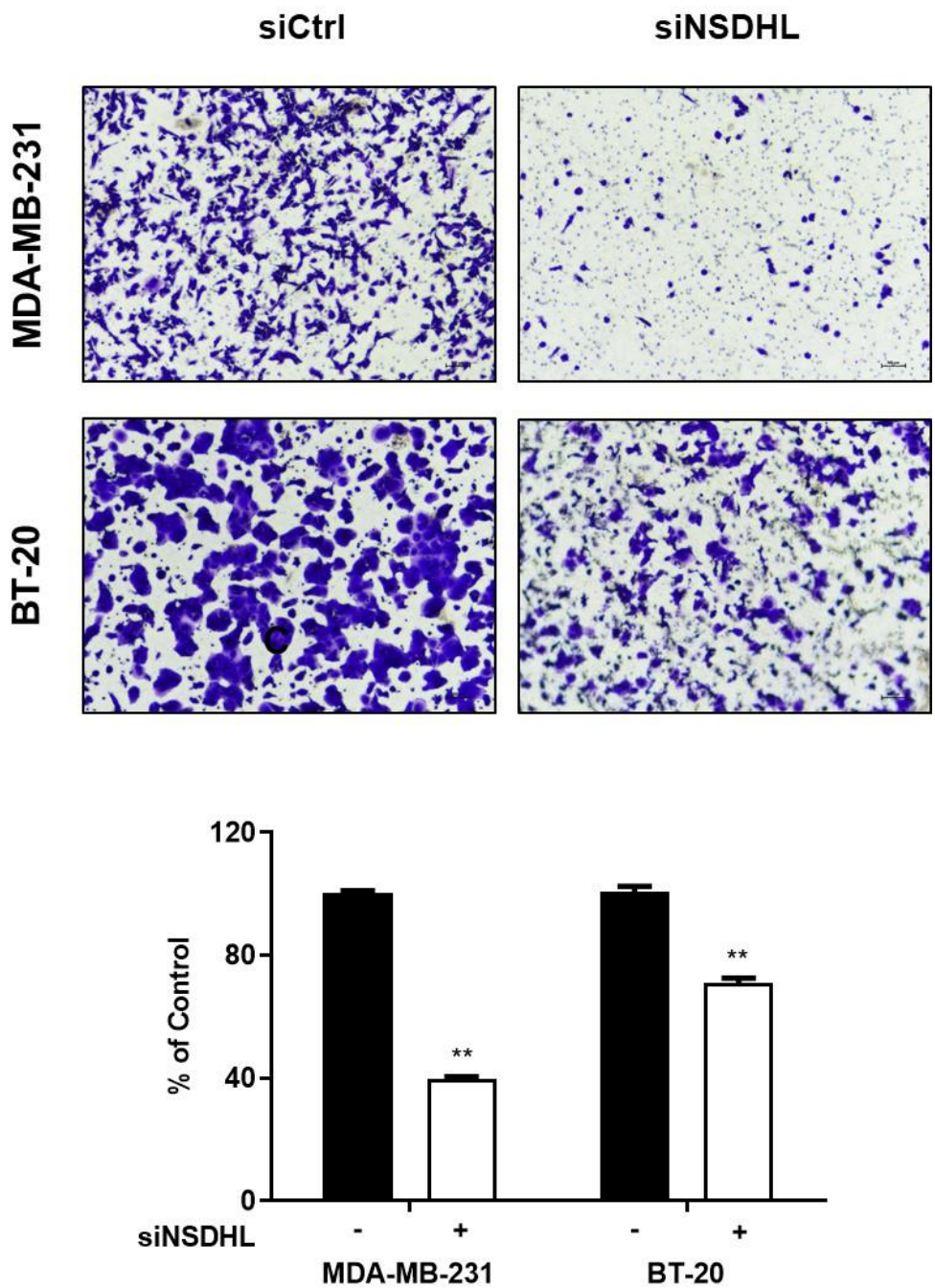
siCtrl
siNSDHL
MDA-MB-231
BT-20
120
80
40
0
% of Control
**
**
siNSDHL
-
+
-
+
MDA-MB-231
BT-20

B

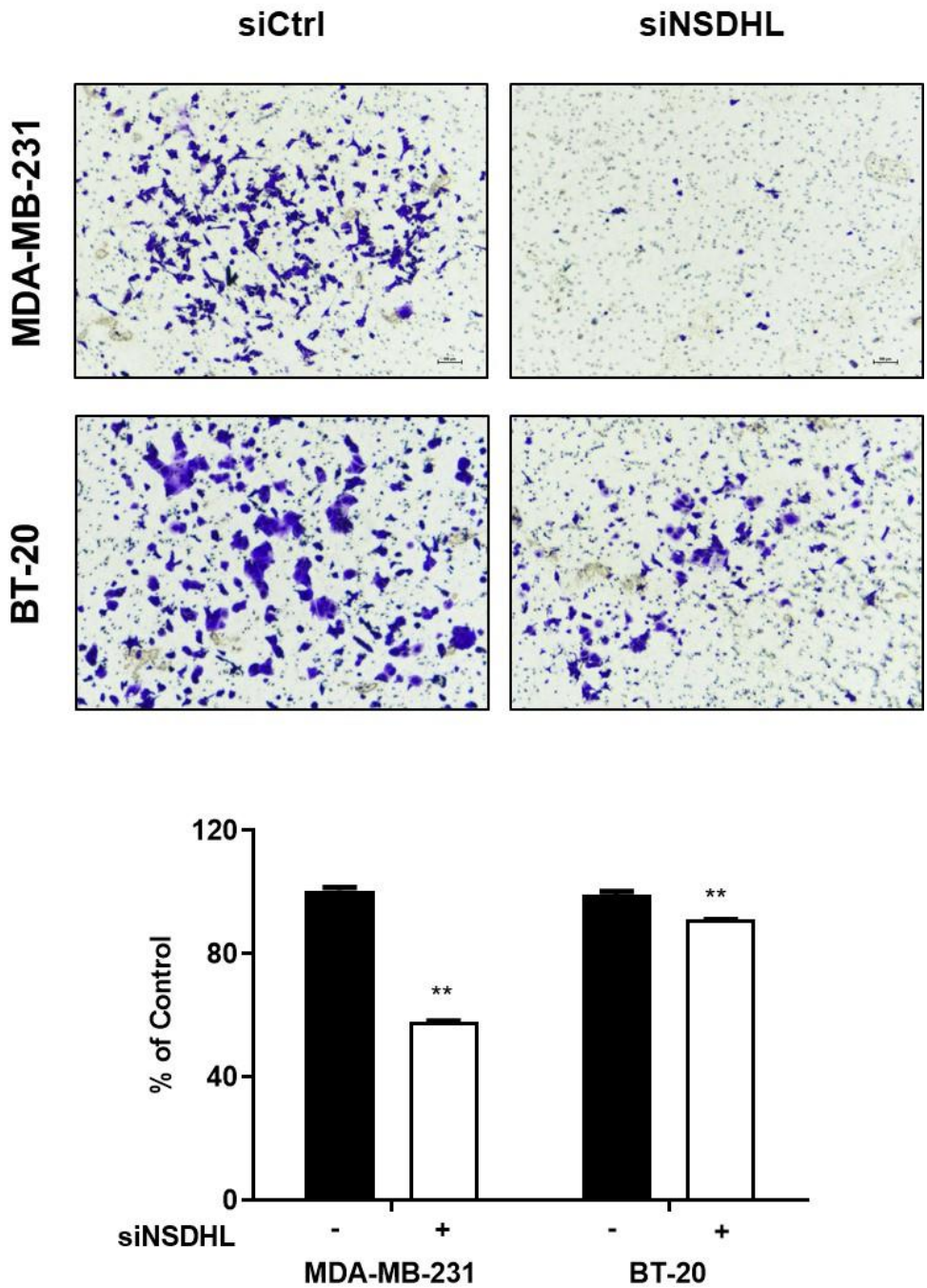
siCtrl
siNSDHL
MDA-MB-231
BT-20
120
80
40
0
% of Control
**
**
siNSDHL
-
+
-
+
MDA-MB-231
BT-20

C

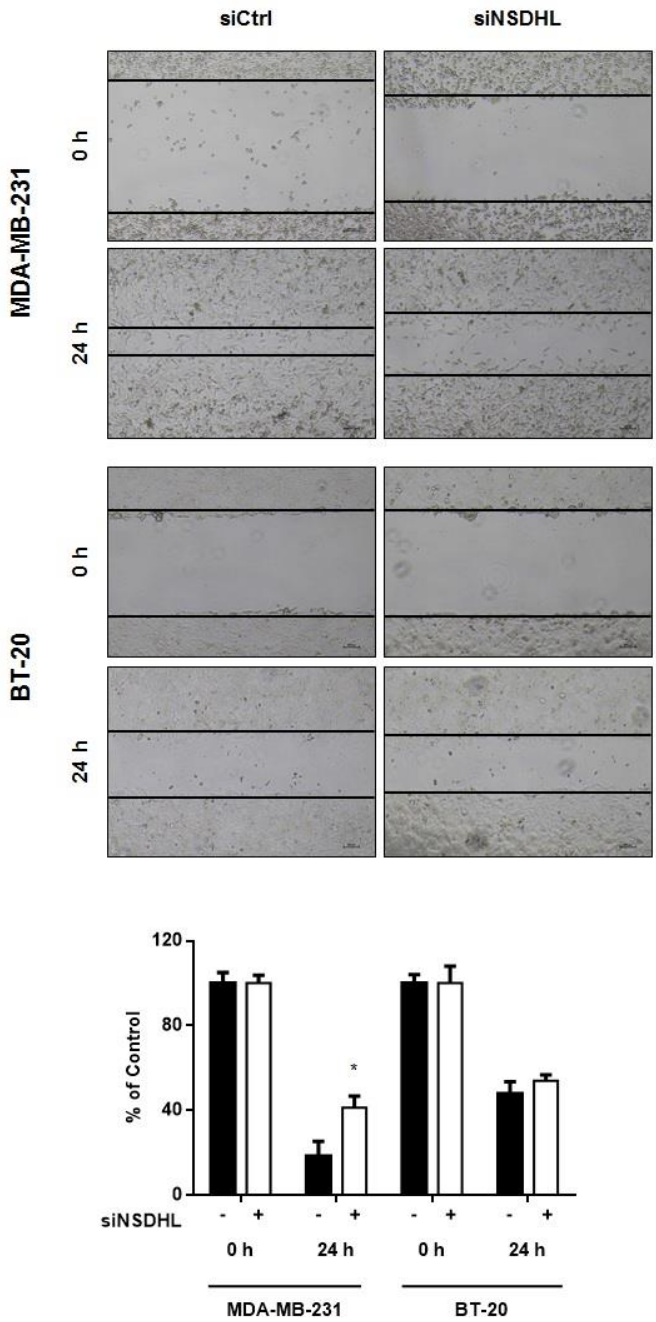
siCtrl
siNSDHL
MDA-MB-231
0 h
24 h
BT-20
0 h
24 h
120
80
40
0
% of Control
*
siNSDHL
- + - + - + - +
0 h
24 h
0 h
24 h
MDA-MB-231
BT-20

Figure 6. *NSDHL* regulated migration and invasion of MDA-MB-231 and BT-20 cells. (A) transwell assay and (B) invasion assay demonstrated that *NSDHL* knock-down inhibited cell migration (x40) in TNBC si treated cells as compared with Control cells. These assays were performed for 24 h (48 h post transfection) to assess cell migration. The migrated cells were stained with crystal violet and imaged by microscopy. The concentration was measured with 10% acetic acid and read by Spectramax 190 (Lm: 570). We compared siNSDHL cells by standardizing siCONTROL to 100%. (C) Consistently, the migration was confirmed in the wound healing assay (x40). The wound was closed slowly in *NSDHL* knock-down of MDA-MB-231 and BT-20 cells. The length of the wound was measured and compared based on control cells. These results showed that *NSDHL* siRNA significantly reduce migration and invasion in TNBC cells. Data were expressed as mean ± standard deviation. Each experiment was done in triplicate. * $p<0.005$; ** $p<0.001$ (Multiple t-test).

5) Effect of *NSDHL* knock-down total cholesterol level in breast cancer cells

NSDHL is involved in cholesterol biosynthesis and cholesterol is related with breast cancer. We measured total cholesterol level in MCF7, MDA-MB231 and BT-20 cells. It was quantified both cholesterol esters and free cholesterol by fluorometric. After 48 hours, *NSDHL* siRNA 20 nM treated cells demonstrated significant reduction in breast cancer cells ($p<0.01$) (Figure 7A), especially in MDA-MB-231 cell. In detail, cholesterol level of BT-20 cell was 90 times higher than MDA-MB-231 and MCF7 cells ($p<0.01$) (Figure 7B). To support these results, we analyzed in western blotting with involved in sterol biosynthesis enzymes. In western blotting assay, we found that binding to specific sterol element, EGFR, SREBP-1 and LDLR expressions were reduced in siRNA transfected cells (Figure 8B). These results were definitely confirmed that *NSDHL* involved in the molecular mechanisms might be associated with cholesterol in breast cancer cells.

A B

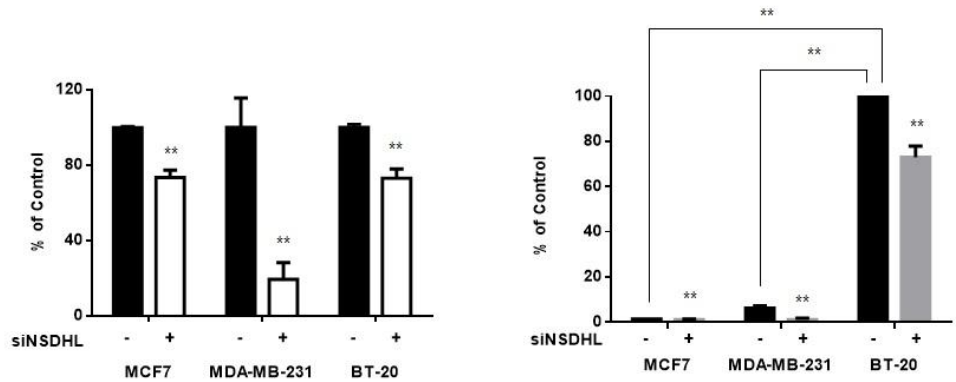

Figure 7. Silencing of *NSDHL* controlled total cholesterol level in breast cancer cells. Decreased total cholesterol level in *NSDHL* knock-down MCF7 and MDA-MB-231 and BT-20 cells. It was quantified both cholesterol esters and free cholesterol by fluorometric. (A) Total cholesterol level regulated by siNSDHL was significantly reduced. (B) In order to confirm the association with cholesterol, we analyzed the amount of cholesterol between MCF7, MDA-MB-231 and BT-20 cells were compared. In detail, total cholesterol level of BT-20 cell was significantly higher than MDA-MB-231 and MCF7 cells. Data were expressed as mean ± standard deviation. Each experiment was done in triplicate. * $p<0.005$; ** $p<0.001$ (Multiple t-test).

6) Predicted Mechanism of *NSDHL* regulation in breast cancer cells

To determine the biological significance of *NSDHL* in breast cancer cells related with EGFR/ biosynthesis pathway of cholesterol, we confirmed by western blotting analysis (Figure 8A, B). In these results, silencing of *NSDHL* decreased whole protein expressions involved in EGFR/biosynthesis pathway related with proliferation and migration.

A

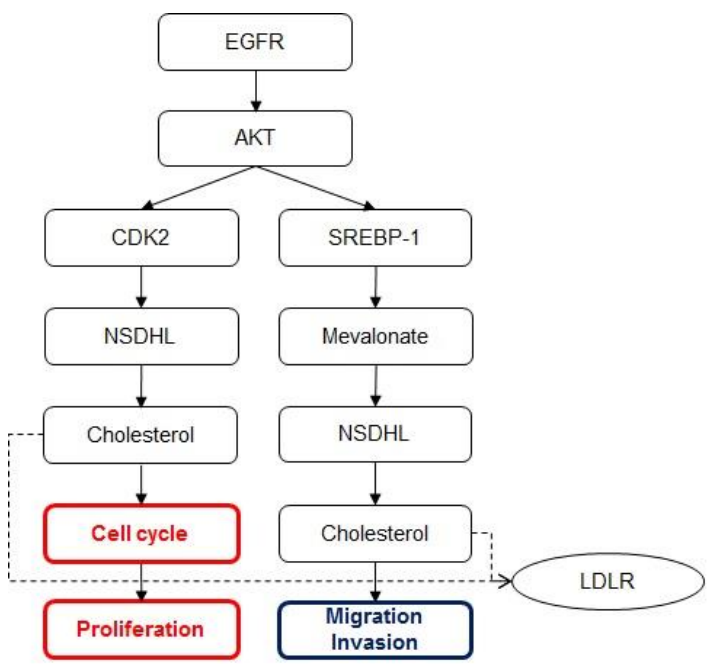

B

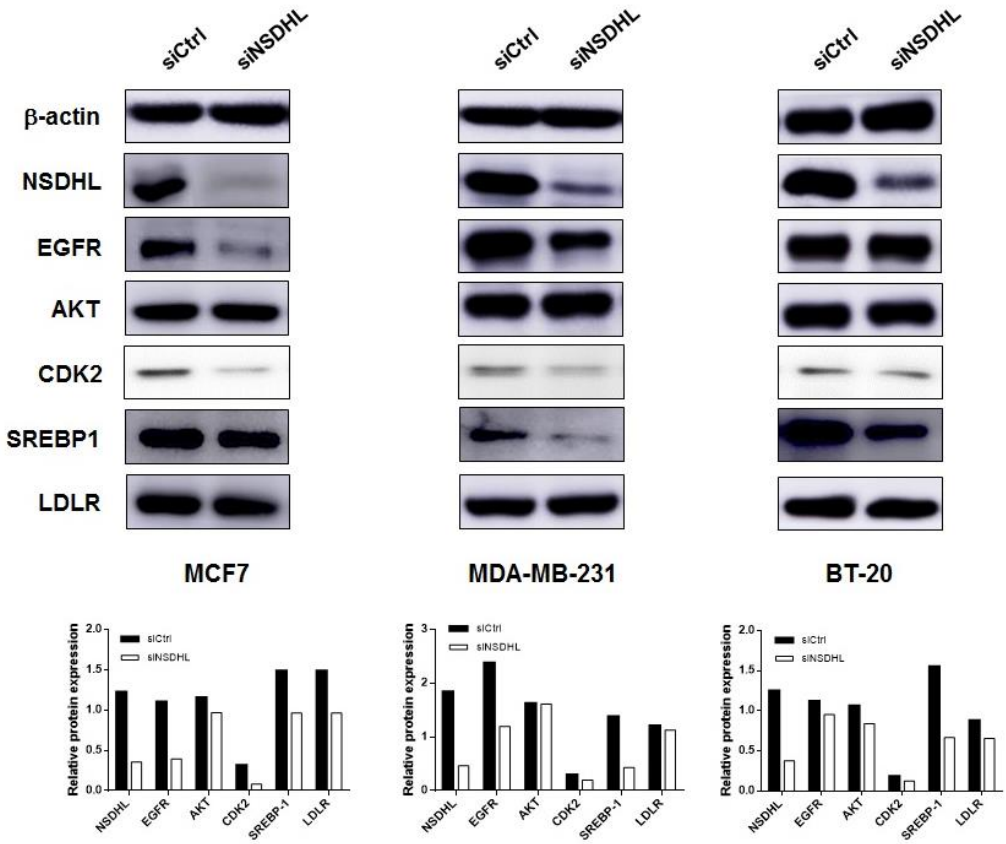

Figure 8. Predicted mechanism of *NSDHL* regulation in breast cancer cells. (A) To determine the biological significance of *NSDHL* in breast cancer cells related with EGFR/ biosynthesis pathway of cholesterol, (B) we confirmed EGFR, AKT, CDK2, SREBP-1 and LDLR expressions by western blotting analysis.

2. *In vivo*

1) Downregulation of *NSDHL* expression in MDA-MB-231 cell by shRNA lentiviral particles transduction

We performed short hairpin RNA (shRNA) lentiviral particles transduction in MDA-MB-231 cell for *in vivo* study. Selected stable clones expression the shRNA via Puromycin dihydrochloride selection were measured mRNA expression levels by RT-qPCR ($p<0.01$) and protein levels in western blot analysis (Figure 9A, B). These results supported that the suppression of *NSDHL* by shRNA could lead to inhibition of MDA-MB-231 cell progression and metastasis in NSG mice.

A B

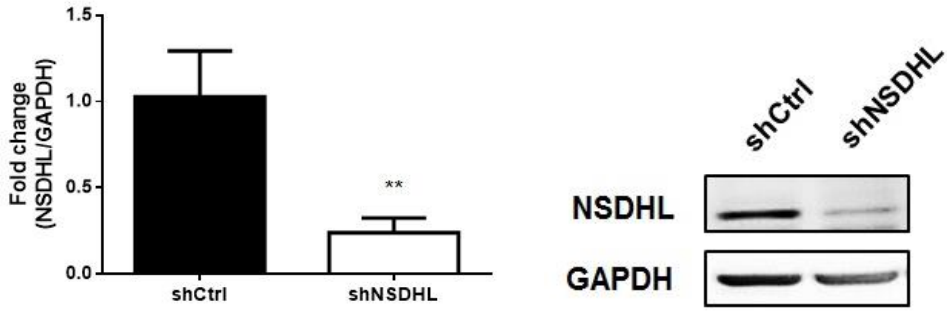

Figure 9. Downregulation of *NSDHL* expression in MDA-MB-231 cell by shRNA lentiviral particles transduction. Selected stable colones were measured mRNA expression levels by (A) RT-qPCR and protein levels in (B) western blot analysis. These results supported that the suppression of *NSDHL* by shRNA could lead to inhibition of MDA-MB-231 cell proliferation. Each experiment was done in triplicate. * $p<0.005$; ** $p<0.001$ (Multiple t-test).

2) Tumor progression and lung metastasis of NSG mouse was decreased by shNSDHL in *in vivo*

NOD/SCID gamma mice born in between july 31, 2018 and august 9, 2018 injected on september 21, 2018. 5 shCONTROL mice and 5 shNSDHL mice were injected into each left breast (Figure 10A). Tumor growth in NSG mice were significantly inhibited by *NSDHL* knock-downed cell for 44 day (p<0.01) (Figure 10B). Also, the control and knock-down tumor were different in volume, weight (p<0.01) and immunohistochemistry (Figure 10C, D and E). Small lung nodules were observed (Figure 11A) and lung parenchyma was replaced with extensive lung metastasis in hematoxylin and eosin staining (H&E staining) (Figure 11B).

A

B

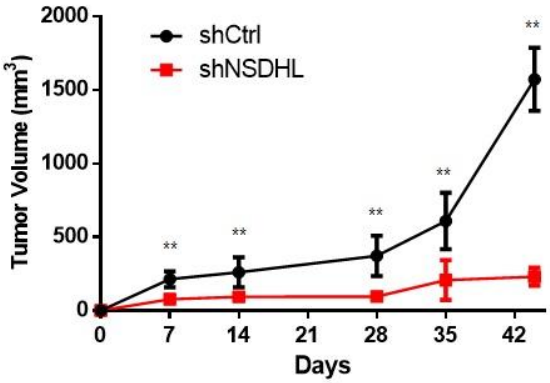
shCtrl
shNSDHL
Tumor Volume (mm3)
2000
1500
1000
500
0
0
7
14
21
28
35
42
Days
**

C

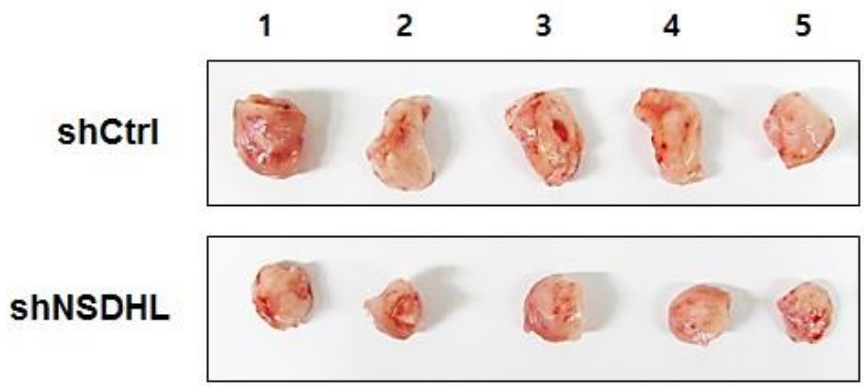
1
2
3
4
5
shCtrl
shNSDHL

D

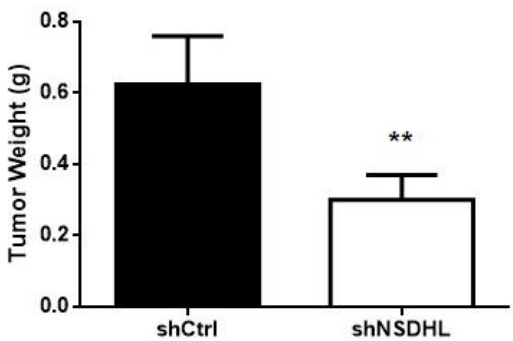
Tumor Weight (g)
0.8
0.6
0.4
0.2
0.0
**
shCtrl
shNSDHL

E

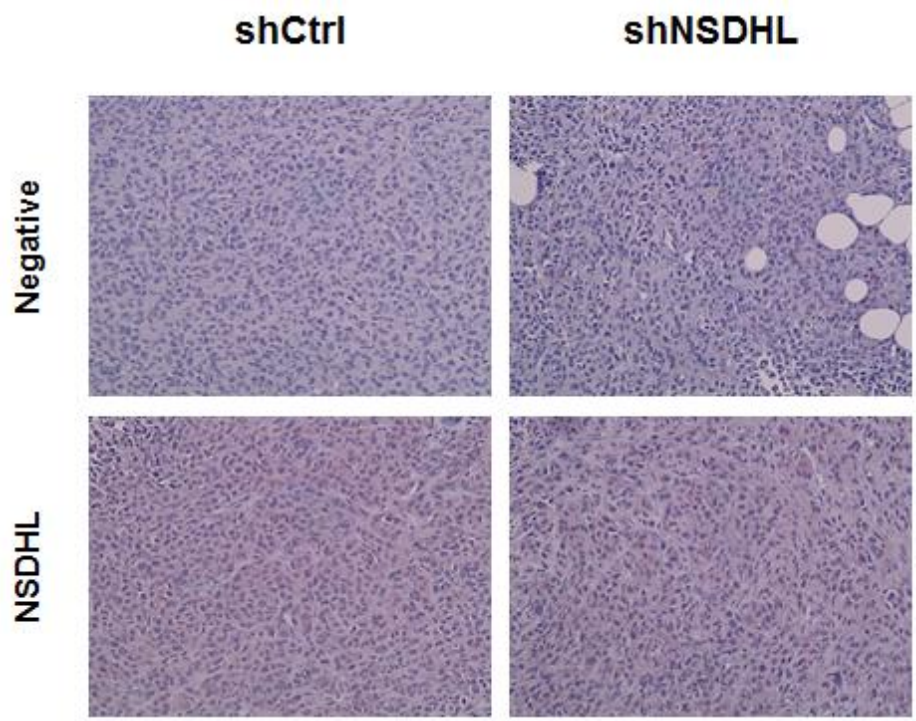

Figure 10. Tumor growth of NSG mouse was inhibited by shNSDHL in *in vivo.* (A), (B) Tumor progression was significantly inhibited by *NSDHL* knock-downed cell for 44 day and the control and knock-down tumor were different in (C) volume, (D) weight and (E) immunohistochemistry. * $p<0.005$; ** $p<0.001$ (Multiple t-test).

A

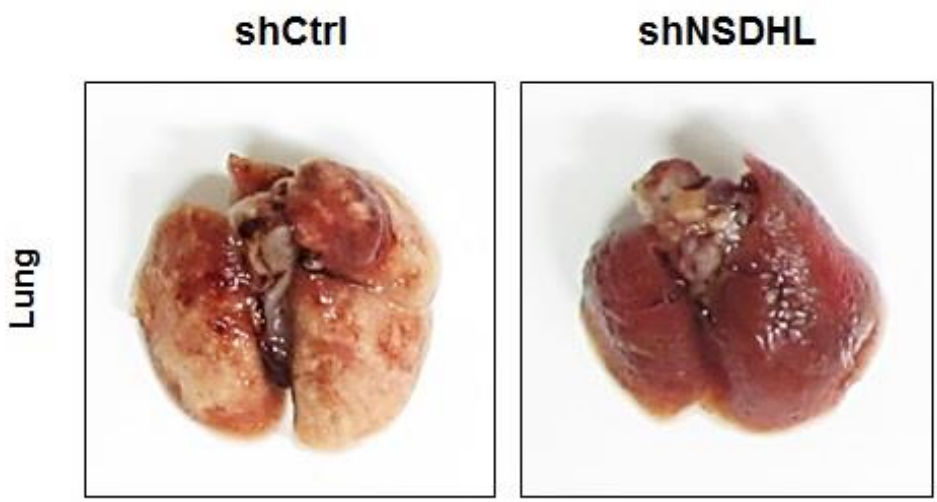

B

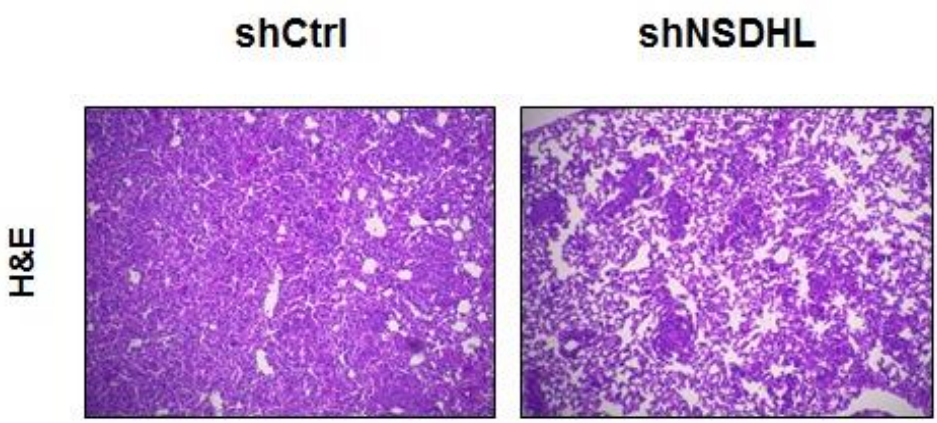

Figure 11. (A) Lung metastasis of NSG mouse was verified with (B) H&E staining

3. Clinical implication of *NSDHL* in breast cancer

As shown in Table 2, 3 and Figure 12, high *NSDHL* expression in a total of 3951 breast cancer patients could be associated with lower recurrence free survival (Hazard Ratio (HR) = 1.419, 95% Confidence Interval (CI) = 1.267 – 1.59, *P*–value (log–rank test) = 1.155×10^{-9}). luminal A (HR = 1.307, 95% CI = 1.103 – 1.55, *P*–value = 0.00197) and TNBC (HR = 1.605, 95% CI = 0.9134 – 2.819, *P*–value = 0.09691) subtypes, such tendency of the reduction in survival was more obvious upon high *NSDHL* expression regarding the *NSDHL* expression in 8 breast cancer cell lines (Figure 2A, B and C).

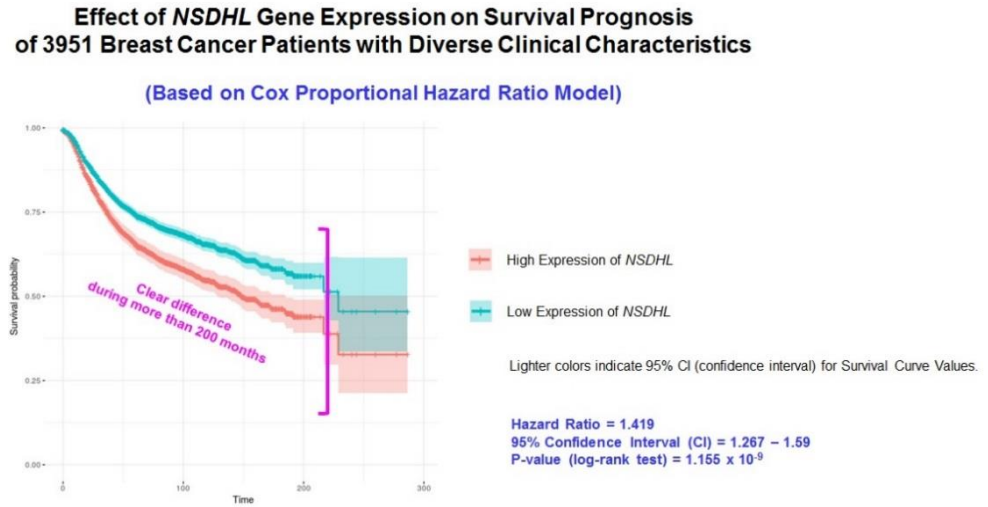

Figure 12. Recurrence free survival data by *NSDHL* expressions in 3951 breast cancer patients

Discussion

NAD(P)−dependent steroid dehydrogenase−like play a critical role in meiosis activation [23]. In the skin, MASs activate because of the skin abnormalities caused by cholesterol synthesis in human and animal, including SC4MOL (sterol−C4−methyl oxidase−like 1) [15, 24] and EGFR may be important in these skin changes in human and animal through EGFR signaling [11, 15, 25]. In addition, inactivation of SC4MOL and *NSDHL* reduced EGFR expression. In many studies, they implicated the function of the cholesterol pathway in tumor grow and response to treatment [15]. For instance, , the sensitivity of neck and head cancer cells in apoptosis [26, 27] and through EGFR signaling, sterol composition of the membrane is regulated [15, 28]. Furthermore, *NSDHL* derived from ER membranes [18], cooperate with lipid rafts to promote metastasis by lipid−depleted serum (LDs) [22]. However, the impact of *NSDHL* on progression and metastasis of breast cancer remained and underlying mechanism is not clearly demonstrated.

We here use a *NSDHL*, which was selected as a therapeutic target, function in breast cancer in *in vitro*, *in vivo* and clinal strategy. Our data imply a important functional role for *NSDHL* in breast cancer and potential biomarker for diagnosis in breast cancer patients. From whole exome sequencing in 120 breast tumor and normal paired tissues, *NSDHL* has 3 mutations and high level in hazard ratio [5].

To investigate the pathological function of *NSDHL* in breast cancer, various experiments were performed in *NSDHL* silenced breast cancer cell lines. In *NSDHL* expression in 8 breast cancer cell line, MCF7, MDA-MB-231 and BT-20 cells were higher than MCF10A cell in both mRNA and protein levels. Then we regulated cells with specific siRNA targeting *NSDHL*. These results revealed that *NSDHL* regulates cell survival, morphogenic differentiation, colony formation and G0/G1, S, G2/M phases of cell cycle in cell proliferation and growth. EGFR is upregulated in non-small-cell lung cancer, metastatic colorectal cancer, glioblastoma, head and neck cancer, pancreatic cancer, and breast cancer. EGFR over-activate downstream signaling pathways, including the RAS-RAF-MEK-ERK MAPK and AKT-PI3K-mTOR pathways, activate chronic initiation and

progression through G1 cell cycle of the cancer cell proliferation [29]. Also, the PI3K/AKT/mTOR pathway, implicated in endocrine resistance, is a major intracellular pathway, which leads to cell proliferation [30, 31]. LDL-cholesterol induced breast cancer cell growth, migration [32] and LDLR accelerates LDL-cholesterol that increased recurrence and mortality in breast cancer [33]. We analyzed the regulation of *NSDHL* and EGFR/AKT/LDLR expressions in protein level and found through this pathway that affected cell growth.

Erlotinib, a small-molecule epidermal growth factor receptor tyrosine kinase inhibitor has potent effect in non-small-cell lung cancer proliferation In that results, H322 NSCLC cells highly expressed EGFR was accompanied by G1/S phase arrest, because of the cell growth inhibition by erlotinib [34]. And regardless of EGFR expression, the ability of erlotinib to inhibit CDK2 activity is important role for cellular sensitivity to erlotinib and the p27 expression in the cytoplasm also involved in erlotinib resistance [35]. Additionally, depletion of SC4MOL and *NSDHL*, sensitizes tumor cells to EGFR inhibitor [15]. Therefore, we tested the sensitivity of erlotinib, a small-molecule EGFR tyrosine kinase inhibitor,

related with *NSDHL* in breast cancer cells. These results also indicated that erlotinib is effectively reduced breast cancer cell growth with *NSDHL* relation to CDK2 protein expression.

In addition, *NSDHL* has impact on metastasis in TNBC cell lines. Specifically, in *NSDHL* induced cells, migration and invasion ability were increased consistent with the degree of wound closer. In previous study, SREBP-1 involved in cholesterol pathway promotes migration and invasion in breast cancer [36]. *NSDHL* translocated to the plasma membrane from the intracellular compartment and promote metastasis relation to LDLR expression relation to LDL-cholesterol [22, 32]. We found that regulated *NSDHL* reduced SREBP-1 and LDLR expression of protein level in breast cancer cells.

We were concerned about the amount of cholesterol in breast cancer, total cholesterol levels were measured in the cells, resulting in a high cholesterol level in order of BT-20, MDA-MB-231 and MCF7 cells. After then, we are going to consider the relationship between EGFR, cholesterol and breast cancer in relation to the amount of cholesterol expressed by EGFR.

To reveal the mechanism of *NSDHL* in cholesterol pathway, we analyzed various enzymes, involved in cholesterol pathway. For example, EGFR, AKT, SREBP-1 and LDLR [37]. As well as we tested CDK2. In previous study, the LDLR expression is stimulated by activated SREBP-1 and in cholesterol homeostasis regulation [38] and SREBP-SCAP complex to move to the Golgi is promoted by activated EGFR/mTOR signaling [37]. In these results, we found out *NSDHL* regulated by EGFR/AKT pathway. And we predicted that *NSDHL* affected to cell cycle and proliferation from CDK2 and translocated to LDLR related with cholesterol. But, in migration and invasion, *NSDHL* was affected by SREBP-1 relation to LDLR.

After then, we confirmed the progression and metastasis ability of *NSDHL* in NSG mice. The downregulation of *NSDHL* induced a decrease in tumor growth and *NSDHL* expression through immunohistochemistry. Also, metastasis in H&E staining of lung was inhibited compared with control cell.

Finally, the Cox proportional hazard ratio model analysis in 3951 breast cancer patients revealed that *NSDHL* is a significantly meaningful gene in breast cancer clinically. Therefore, these results indicated that *NSDHL* is a pivotal molecule for prognosis in breast cancer.

In conclusion, we first identified the function of *NSDHL* gene in breast cancer to help the proliferation and metastasis of breast cancer cells and showed the possibility as a therapeutic target.

References

1. Jung, K.W., et al., *Cancer Statistics in Korea: Incidence, Mortality, Survival, and Prevalence in 2015.* Cancer Res Treat, 2018. **50**(2): p. 303-316.
2. Jung, K.W., et al., *Cancer statistics in Korea: incidence, mortality, survival, and prevalence in 2011.* Cancer Res Treat, 2014. **46**(2): p. 109-23.
3. WHOG. *stimated Cancer Incidence, Mortality and Prevalence Worldwide in 2012.* 2012; Available from: http://info.cancerresearchuk.org/cancerstats/world/.
4. Hurvitz, S.A., et al., *Current approaches and future directions in the treatment of HER2-positive breast cancer.* Cancer Treat Rev, 2013. **39**(3): p. 219-29.
5. Jung, S.-Y., *Detection of functional variants using exome sequencing and gene expression profiling in breast cancer*. February, 2015.
6. *NSDHL From Wikipedia, the free encyclopedia*.
7. Cowey, S. and R.W. Hardy, *The metabolic syndrome: A high-risk state for*

cancer? Am J Pathol, 2006. **169**(5): p. 1505-22.

8. Llaverias, G., et al., *Role of cholesterol in the development and progression of breast cancer.* Am J Pathol, 2011. **178**(1): p. 402-12.

9. McDonnell, D.P., et al., *Obesity, cholesterol metabolism, and breast cancer pathogenesis.* Cancer Res, 2014. **74**(18): p. 4976-82.

10. McMillan, D.C., N. Sattar, and C.S. McArdle, *ABC of obesity. Obesity and cancer.* BMJ, 2006. **333**(7578): p. 1109-11.

11. Gabitova, L., et al., *Endogenous Sterol Metabolites Regulate Growth of EGFR/KRAS-Dependent Tumors via LXR.* Cell Rep, 2015. **12**(11): p. 1927-38.

12. Gorin, A., L. Gabitova, and I. Astsaturov, *Regulation of cholesterol biosynthesis and cancer signaling.* Curr Opin Pharmacol, 2012. **12**(6): p. 710-6.

13. Guo, D., et al., *An LXR agonist promotes glioblastoma cell death through inhibition of an EGFR/AKT/SREBP-1/LDLR-dependent pathway.* Cancer Discov, 2011. **1**(5): p. 442-56.

14. Acimovic, J. and D. Rozman, *Steroidal triterpenes of cholesterol synthesis.* Molecules, 2013. **18**(4): p. 4002-17.

15. Sukhanova, A., et al., *Targeting C4-demethylating genes in the cholesterol pathway sensitizes cancer cells to EGF receptor inhibitors via increased EGF receptor degradation.* Cancer Discov, 2013. **3**(1): p. 96-111.

16. Nes, W.D., *Biosynthesis of cholesterol and other sterols.* Chem Rev, 2011. **111**(10): p. 6423-51.

17. Lingwood, D. and K. Simons, *Lipid Rafts As a Membrane-Organizing Principle.* Science, 2010. **327**(5961): p. 46-50.

18. Zweytick, D., K. Athenstaedt, and G. Daum, *Intracellular lipid particles of eukaryotic cells.* Biochim Biophys Acta, 2000. **1469**(2): p. 101-20.

19. Caldas, H. and G.E. Herman, *NSDHL, an enzyme involved in cholesterol biosynthesis, traffics through the Golgi and accumulates on ER membranes and on the surface of lipid droplets.* Hum Mol Genet, 2003. **12**(22): p. 2981-91.

20. Goodman, J.M., *Demonstrated and inferred metabolism associated with*

cytosolic lipid droplets. J Lipid Res, 2009. **50**(11): p. 2148-56.

21. Ohashi, M., et al., *Localization of mammalian NAD(P)H steroid dehydrogenase-like protein on lipid droplets.* J Biol Chem, 2003. **278**(38): p. 36819-29.

22. Xue, T., et al., *Proteomic Analysis of Two Metabolic Proteins with Potential to Translocate to Plasma Membrane Associated with Tumor Metastasis Development and Drug Targets.* Journal of Proteome Research, 2013. **12**(4): p. 1754-1763.

23. Sharpe, L.J. and A.J. Brown, *Controlling cholesterol synthesis beyond 3-hydroxy-3-methylglutaryl-CoA reductase (HMGCR).* J Biol Chem, 2013. **288**(26): p. 18707-15.

24. He, M., et al., *Mutations in the human SC4MOL gene encoding a methyl sterol oxidase cause psoriasiform dermatitis, microcephaly, and developmental delay.* J Clin Invest, 2011. **121**(3): p. 976-84.

25. Cunningham, D., et al., *Analysis of hedgehog signaling in cerebellar granule cell precursors in a conditional Nsdhl allele demonstrates an*

essential role for cholesterol in postnatal CNS development. Hum Mol Genet, 2015. **24**(10): p. 2808-25.

26. Bionda, C., et al., *Differential regulation of cell death in head and neck cell carcinoma through alteration of cholesterol levels in lipid rafts microdomains.* Biochem Pharmacol, 2008. **75**(3): p. 761-72.

27. Kalinowski, F.C., et al., *Regulation of epidermal growth factor receptor signaling and erlotinib sensitivity in head and neck cancer cells by miR-7.* PLoS One, 2012. **7**(10): p. e47067.

28. Sigismund, S., et al., *Clathrin-mediated internalization is essential for sustained EGFR signaling but dispensable for degradation.* Developmental Cell, 2008. **15**(2): p. 209-219.

29. Wee, P. and Z. Wang, *Epidermal Growth Factor Receptor Cell Proliferation Signaling Pathways.* Cancers (Basel), 2017. **9**(5).

30. Paplomata, E. and R. O'Regan, *The PI3K/AKT/mTOR pathway in breast cancer: targets, trials and biomarkers.* Ther Adv Med Oncol, 2014. **6**(4): p. 154-66.

31. Simigdala, N., et al., *Cholesterol biosynthesis pathway as a novel mechanism of resistance to estrogen deprivation in estrogen receptor-positive breast cancer.* Breast Cancer Research, 2016. **18**.

32. dos Santos, C.R., et al., *LDL-cholesterol signaling induces breast cancer proliferation and invasion.* Lipids Health Dis, 2014. **13**: p. 16.

33. Gallagher, E.J., et al., *Elevated tumor LDLR expression accelerates LDL cholesterol-mediated breast cancer growth in mouse models of hyperlipidemia.* Oncogene, 2017. **36**(46): p. 6462-6471.

34. Ling, Y.H., et al., *Erlotinib, an effective epidermal growth factor receptor tyrosine kinase inhibitor, induces p27KIP1 up-regulation and nuclear translocation in association with cell growth inhibition and G1/S phase arrest in human non-small-cell lung cancer cell lines.* Mol Pharmacol, 2007. **72**(2): p. 248-58.

35. Yamasaki, F., et al., *Sensitivity of breast cancer cells to erlotinib depends on cyclin-dependent kinase 2 activity.* Mol Cancer Ther, 2007. **6**(8): p. 2168-77.

36. Bao, J., et al., *SREBP-1 is an independent prognostic marker and promotes invasion and migration in breast cancer.* Oncol Lett, 2016. **12**(4): p. 2409-2416.

37. Gabitova, L., A. Gorin, and I. Astsaturov, *Molecular Pathways: Sterols and Receptor Signaling in Cancer.* Clinical Cancer Research, 2014. **20**(1): p. 28-34.

38. Guo, D.L., et al., *EGFR Signaling Through an Akt-SREBP-1-Dependent, Rapamycin-Resistant Pathway Sensitizes Glioblastomas to Antilipogenic Therapy.* Science Signaling, 2009. **2**(101).

요약 (국문초록)

연구목적: 본 연구에서는 유방암 환자의 암 조직과 정상조직 및 혈액에서 전엑솜 서열 분석을 통해 발굴한 콜레스테롤 생합성에 관여하는 *NSDHL* 유전자의 발현을 유방암세포에서 조절한 후 세포실험과 동물실험에서 증식과 전이에 미치는 영향과 그 기전을 확인하여 임상적으로 적용 가능성이 있는 기초 연구를 진행하고자 하였다.

연구방법: 유방암세포에서의 *NSDHL* 유전자의 발현을 확인하기 위해 Western blotting, SYBR™ Green Real-Time PCR을 사용하였고, *NSDHL* 넉다운 세포를 형성하기 위해 Lipofectamine 2000™을 사용하여 세포에 siRNA를 형질주입하였다. 그리고 세포 증식, 3D culture, 콜로니 형성, 세포주기, 전이, 침윤, 상처 치유 분석 및 콜레스테롤 분석 등 다양한 기능적 연구를 수행하였다. 또한 erlotinib을 처리하여 *NSDHL* 유전자의 표적 약물로서 치료에 효과적이라는 것을 확인하였다. 마지막으로 MDA-MB-231에 *NSDHL*의 shRNA를 형질도입시키고 NSG 마우스에서 *NSDHL* 능력을 확인하였다. 임상적으로 마이크로 어레이 유전자 발현 데이터와 Gene expression omnibus (GEO) 데이터베이스에 등록된 임상 데이터를 사용하여 이전의 연구에서

사용된 *NSDHL* 발현의 생존율에 대한 콕스 비례 위험률 모델 분석을 시행하였다.

연구결과: 정상 유방암세포 (MCF10A)보다 luminal A (MCF7)와 삼중 음성 유방암세포 (MDA-MB-231, BT-20)에서의 *NSDHL* mRNA와 단백질 발현이 모두 높게 나타났다. siRNA에 의한 *NSDHL* 발현 조절은 증식을 감소시키고 (p<0.01), 유방암세포에서의 분화 및 erlotinib에서의 민감성을 감소시켰다. 또한 *NSDHL*은 특히 MDA-MB-231 세포에서 TNBC의 이동과 침입을 억제했다 (p<0.01). 또한, *NSDHL*이 콜레스테롤 수치를 조절함을 알아냈다. 이를 우리는 생체 내 실험에서 *NSDHL*이 종양 진행 (p<0.01), 전이를 조절함을 관찰하면서 다시 한번 *NSDHL* 유전자의 기능을 확인하였다. 또한, 총 3951명의 유방암 환자에서 높은 *NSDHL*의 발현은 낮은 재발 생존율과 관련이 있을 수 있으며 임상적으로 의미 있는 유전자임을 확인하였다.

결론: 결론적으로, 유방암에서 *NSDHL* 유전자가 유방암 세포의 증식과 전이를 돕는 기능을 처음으로 밝히고, 이를 치료의 표적으로 사용할 수 있는 가능성을 보였다.

주요어: 유방암, *NSDHL*, 넉다운, 증식, 전이, 콜레스테롤, EGFR

학 번: 2017-23758